CHARACTERIZATION OF BORON NITRIDE THIN FILMS ON SILICON (100) WAFERS

Walter Maranon, B.E.

Thesis Prepared for the Degree of

MASTER OF SCIENCE

UNIVERSITY OF NORTH TEXAS

August 2007

APPROVED:

Seifollah Nasrazadani, Major Professor
Shuping Wang, Committee Member
Mitty Plummer, Committee Member
Mike Kozak, Program Coordinator
Nourredine Boubekri, Chair of the Department of Engineering Technology
Oscar Garcia, Dean of the College of Engineering
Sandra L. Terrell, Dean of the Robert B. Toulouse School of Graduate Studies

Maranon, Walter. Characterization of boron nitride thin films on silicon (100) wafer. Master of Science (Engineering Technology), August 2007, 69 pp, 12 tables, references, 47 titles.

Cubic boron nitride (cBN) thin films offer attractive mechanical and electrical properties. The synthesis of cBN films have been deposited using both physical and chemical vapor deposition methods, which generate internal residual, stresses that result in delamination of the film from substrates. Boron nitride films were deposited using electron beam evaporation without bias voltage and nitrogen bombardment (to reduce stresses) were characterize using FTIR, XRD, SEM, EDS, TEM, and AFM techniques. In addition, a pin-on-disk tribological test was used to measure coefficient of friction. Results indicated that samples deposited at 400°C contained higher cubic phase of BN compared to those films deposited at room temperature. A BN film containing cubic phase deposited at 400°C for 2 hours showed 0.1 friction coefficient.

ACKNOWLEDGEMENTS

I take this opportunity to express my deep regards to my committee chair Dr. Seifollah Nasrazadani for his guidance and support during the completion of this research work. I would also like to thank my other committee members Dr. Shuping Wang and Dr. Mitty Plummer for their support and encouragement to improve this work.

I like to thank all my colleagues Haritha Namduri, Anjana Rajendran, Kristopher Maheak and Junyeon Hwang for their co-operation without which this research would not have been completed. On a more personal level I want to thank Vanesa for having faith and giving me courage and my family for their moral support.

TABLE OF CONTENTS

Page

LIST OF FIGURES

LIST OF TABLES

CHAPTER I

INTRODUCTION

The science and technology of thin films continue to change at a rapid rate. New materials, processes and applications are reported on a daily basis. The time from discovery to commercialization is often measured in months, which makes the thin films technology an interesting field to develop or combine new methods to achieve better materials (Glocker & Ismat Shah, 1995).

Methods to obtain thin films have evolved into a sophisticated set of techniques used to fabricate many semiconductor devices and tools. Among the applications are very large scale integrated (VLSI) circuits; electronics packaging, sensors, and devices; optical films and devices; as well as protective and decorative coatings. However, the main research has been conducted in the electronic industry (Elshabini Riad & Barlow, 1998).

The method of deposition, the substrate materials, the rate of deposition, and the background pressure influence the thin film properties. Specific applications in modern technology demand such film properties as high optical reflection/transmission, hardness, adhesion, nonporosity, high mobility of charge carriers/insulating properties, chemical inertness toward corrosive environments, stability with respect to temperature, stoichiometry, and orientation in single crystal films. The method to achieve the thin film can be selected based on the properties and applications desired for the material (George, 1992).

Physical vapor deposition (PVD) and chemical vapor deposition (CVD) are the most commonly used methods to grow thin films onto substrate surfaces. Both methods are usually carried in a vacuum environment to control reactions during the process of deposition. During a PVD process a solid or liquid material is vaporized and transported through a vacuum environment to be condensed onto the substrate surface. PVD processes are frequently used to

obtain multilayer coatings. If the material deposited is the product of a chemical reaction, the process is a CVD process. In the effort to design and improve materials, a combination of both methods are used such that optimal results are achieved (Freund & Suresh, 2003).

Cubic boron nitride (cBN) has significant technological potential for thin-films applications in the coating industry. Having a Vickers hardness of about 500 kg/mm^2, cBN is second in hardness only to diamond and hence is a natural candidate for hard, protective coatings. The fact that cBN does not react readily with ferrous metals, can be deposited in thin-film form at low temperatures, and has a high resistance to oxidation makes it even more attractive for tooling applications (Mirkarimi, McCarty & Medlin, 1997).

In the electronics field, cBN has unusual properties such as a wide ban gap (6.3e.V), chemical inertness and high thermal conductivity. Cubic boron nitride is more easily doped to form both n-type as well as p-type semiconductors than diamond. All these properties make cBN a promising semiconductor material that can be used in electronic and optoelectronic devices that operate at high temperature (Deng & Cheng, 2005). The hardness of cBN, second to diamond, makes it an attractive material for mechanical applications (Le & Oechsner, 2003).

Properties of cBN make it an important material in mechanical and electronic applications for tool inserts as in field emission devices. The significance of the study for the cutting tool industry is to expose the tool to higher temperatures and to work with harder materials increasing the tool life time, cutting costs and improve quality products. In the electronics field, the cBN depositions will increase the use of field emission devices in different environments and applications as in cell phones, television screens or any type of electronic display, with better performance, longer life time and display flexibility.

Many attempts were made to obtain cBN using CVD but high content of hexagonal boron nitride (hBN) was found in the deposition. Although cBN was deposited using PVD, high residual stress in the growth process caused a later delamination of the material from the substrate (Chowdhury & Pal, 2004). The delamination is induced by mechanical deformation, damage of failure due the internal stresses, also influencing electrical or magnetic properties in functional devices (Freund & Suresh, 2003). Humidity was reported as one of the causes that initiate delamination of cBN (Moller, Reiche, Bobeth & Pompe, 2002).

PVD has been used more than CVD, and the successful deposition of more than 1 μm of thickness was reported. However, the challenge still remains in reducing residual stresses, poor adhesion and lack of long-term stability with an economic method able to be incorporated to new and challenging applications (Chowdhury & Pal, 2004).

In this investigation, efforts were spent to characterize BN films deposited on silicon (100) wafer using e-beam evaporation without nitrogen bombardment and bias voltage. Deposition of BN films using light condition (lower substrate temperature, no physical bombardment, etc.) should lead to minimal residual stresses generation and hence optical film performance.

CHAPTER II

LITERATURE REVIEW

Physical Vapor Deposition

Physical vapor deposition (PVD) processes work by vaporizing a material from its original state, solid or liquid, into atoms or molecules in a vacuum environment to be condensed onto the substrate surface. Most PVD processes are used to achieve thin film deposition in the range of nanometers in single or multilayers (M.D. Mattox, 1998). Among the most common processes used are the thermal vaporization, sputtering, arc vapor deposition and ion plating.

Thermal Vaporization

Vaporization process.

Material to be deposited must be heated to a temperature where the vapor pressure of the material is appropriate to perform the deposition. Common heating techniques for evaporation/sublimation include resistive heating, high energy electron beams, low energy electron beams and inductive (rf) heating (M.D Mattox, 1998). Materials to be deposited are completely or partially vaporized depending of the application. The most used method for material with low vaporization temperature, below 1500^{o}C, is resistive heating while focused electron beams are used for material deposition above 1500^{o}C (M.D Mattox, 1998).

Three most important parameters during the deposition include pressure, mean free path (MFP) and the ratio from a film vapor arrival and the reactive gas impingement. The relation between pressure, MFP and ratio is illustrated in Table 1.

Table 1. Effect of vacuum pressure over ratio deposition, (A. E. Riad and F. D. Barlow III, Thin film Technology Handbook, MCGraw-Hill, NY (1998)).

Pressure (Torr)	Mean free path	Ratio

10^{-1}	0.5 mm	0.0001
10^{-2}	5 mm	0.001
10^{-3}	5 cm	0.01
10^{-4}	50 cm	0.1
10^{-5}	5 m	1
10^{-6}	50 cm	10
10^{-7}	500 m	100
10^{-8}	5 km	1000
10^{-9}	50 km	10000

The mean free path has been suggested to be ten times the distance from the source to the substrate. When the distance from source to substrate is increased the pressure will decrease otherwise the evaporant will have more interaction with the residual gas which usually is water vapor. Increasing the distance from the source to substrate also means to increase the position rate to maintain the arrival rate ratio (Glocker & Ismat Shah, 1995).

The necessary energy for vaporization is the same for sputtering though the mechanism involved are different. Vaporization energy consists of the following elements:

1. Latent heat to elevate the temperature to the point of material phase change.
2. Enthalpy phase change, this is the dominant energy to change the phase.
3. Kinetic energy to make the vapor phase change.

The evaporation process is the phase change of the material by heating it up from solid to vapor. In thin film processes the temperature to reach this state is less than nominal melting temperature, effective at one atmosphere, due the difference in pressure of the vapor to the material surface which is 0.1-1Torr (Glocker & Ismat Shah, 1995).

Substrate holders for vapor depositions.

The objective of having different holders is to assest the uniformity of the film. Among the types of holders are flat plate, domes, planetary and drums. The most common is the flat plate which is inexpensive and achieves uniformity of ±10%. Domes eliminate geometric distribution errors and achieve a non-uniformity of ± 5%. Planetary holders produce films with a uniformity of ±1%, which is implies a lost of material. The uniformity of coatings prepared using drums is close to flat and frequently used for decorative coatings (Glocker & Ismat Ishah, 1995).

Vapor flux distribution.

For low vaporization rates the flux can be described by a cosine distribution for a point source. Ideally the deposition occurs without colliding, traveling in straight line from the source to the substrate. The distribution depends mainly on source geometry and the evaporant flux, which is treated as a series of cosine (∅) point sources. The ideal emitter has a flux of:

$$f(\phi) = \cos(\phi)$$

In the case of an isotropic deposition, the cosines sum produces a uniform flux in all directions, Figure 1 (Glocker & Ismat Shah, 1995).

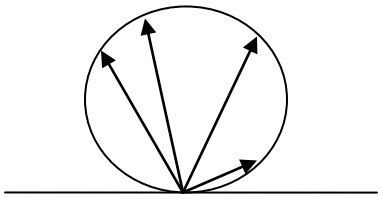

Figure 1. Flux distribution.

Film thickness is affected by the flux distribution combined with the source to substrate distance and the angle of incidence on the substrate. The distance effect from source to substrate on film thickness is accurately described by an inverse distance square. Thus, the farther the substrate is placed from the source, the more uniform the distribution, nevertheless, the

deposition rate falls as the square distance increase described below (Glocker & Ismat Shah, 1995). R is the deposition rate and d the distance.

$$R = \frac{1}{d^2}$$

Resistance Evaporation

The most common way to evaporate a material is through the contact of heated material, which was the first film deposition technique. The process is done by applying current to a material typically tungsten, tantalum, molybdenum, carbon and BN/TiB_2. Although replaced by modern techniques such as electron beam or sputtering, resistance evaporation still finds applications due its reliability and economy (Glocker & Ismat Shah, 1995 and Mattox, 1998).

Electron Beam Evaporation

The difference between a resistance and electron beam evaporations is the heating energy that is applied by the kinetic energy of a high energy current electron beam to the material that is contained in a water cooled cavity or hearth (Graper, 1995). This *e-beam* is used to evaporate refractory materials such as most ceramics, glasses and carbon (Mattox, 1998).

The bent beam evaporation process is commonly used in the thin film production for electronics and optics. L. Holland was the first to initiate research in to this field followed by Hugh Smith and Charles Hanks by designing the 270^o gun for Temescal Corporation. In 1960s and 1970s, electron beam guns were used for aluminum metallization of semiconductors and were later replace by magnetron sputtering. Presently, the wide spread application of multilayer hard coating optical systems has increased the use of the electron beam evaporation process (Graper, 1995).

The electron beam gun works by applying a high energy electron beam produced by a thermionic-emitting filament at high voltage in the range of 10-20 kV to accelerating the

electrons. Magnetic fields focus and deflect the beam onto the surface to be evaporated. Electron beam guns usually operated between 10-50 kW. High power e-beam sources had been reported to vaporize 10-15 kilograms of aluminum obtaining depositions as high as 50 microns per second. The architecture of most guns is vertical but high rate sources were made that deposited in the horizontal direction (Mattox, 1998).

Electron beams are magnetically deflected through 180^{o} to avoid the deposition of material over the filaments. The material to be deposited is contained in crucibles which are water cooled. Some e-beam guns use the option to have multiple pockets to deposit different materials from the same electron source (M.D. Mattox, 1998).

Evaporation kinetics.

A source in high technology thin film fabrication has three sections: the electron gun, the beam magnetic lens and the pocket or hearth containing the material. The basic vaporization process starts at the gun where the beam is formed, passes through the magnetic lens, which focuses the beam over the material. The relationships governing this procedure are:

1. The energy balance of the evaporant charge and the requirement for stable dissipation of the beam energy.
2. The complex distribution of the vapor flux from the evaporant surface caused by the pressure within this vapor and the resultant evaporant surface geometry.
3. The ionizing effect of the electron beam, as it passes through the evaporant vapor cloud, impacts the melt surface and is partially reflected from that surface.

The evaporation process begins when the pressure from the evaporant is greater than 10^{-1} Torr. Increasing the deposition rate requires decreasing the chamber pressure. The accelerating voltage for the electron beam is normally in the range of the 10kV with a current of 1.5A. The

electron beam impacts an area of ¼ to 1cm^2 with energy up to 60 kW/cm^2. For the evaporation to be stable a thermal equilibrium has to exist, energy dissipation has to be stable. The surface absorbs energy from the 10kV electron beam upon impact. The temperature rises to a level such that the evaporation process starts at a pressure of 10^{-4}Torr. The evaporation rate increases until the viscous flow ranges reached and the mean free path is reduced. The evaporation rate increases exponentially until the vapor density is over the evaporant (Graper, 1995).

Sputtering

Sputtering can be defined as the erosion of a material by the continuous ion bombarment. Electron, photons and neutral particles can be used in the evaporation process. Many applications of sputtering include condensation of the ejected particles on a substrate as a thin film. Low energy sputtering applications include milling, etching, thinning and polishing of microstructures. Sputtered particles can be analyzed to determine contaminants of selected sources in cleaning processes. The sputtering process offers advantages over evaporation process due to having particles with kinetic energy that is 3-5 eV above evaporation energy. Kinetic energy helps the particles mobility to produce a smooth and conformal surface. Another advantage is the source area to be evaporated, which improves the film thickness (Mahan, 2000).

Arc Vapor Deposition

Arc vapor deposition uses an electrode under arcing conditions to vaporize material. High current with low voltage passing through a gas produces the evaporation. The arc has to be close the ionization potential of the gas. The electrode surfaces are vaporized and form plasma to then be deposited on the surface of the substrate. Arc vapor deposition processes were first used to deposite carbon and metal films; carbon depositions were used as a replication film in electron microscopy (Mattox, 1998).

Ion Platin g

Phase	a(Å)	c(Å)	Space	Atom positions

Ion assisted deposition (IAD) is a deposition process where the substrate and the growing film is under continuous bombardment with energetic particles to produce changes in the material being deposited. Although, the deposition mechanism is not clear, the main aspect of this process is the high bombardment of ions into the surface (M.D. Mattox).

Boron Nitride

Boron, carbon and nitrogen are neighbor elements which are basic components for super hard thin films and thin systems with interesting applications due their electrical and mechanical properties. One of these combinations is the stoichiometric boron nitride, which forms different microstructures with different properties (Ullmann, Baglin & Kellock, 1997 and Linss et al., 2004).

Boron nitride, like carbon forms four crystalline structures: cubic (cBN), wurzite (wBN), hexagonal (hBN) and rhombohedral (rBN), the crystal structure and phases are described in Table 2 and Figure 2 (Mirkarimi et al., 1997).

			group	
hBN	2.5043	6.6562	$P6_3mm$	B:(0,0,0), (2/3,1/3,1/2),
				N(2/3, 1/3,0), (0,0,0)
rBN	2.5042	9.99	R3m	B:(0,0,0), (2/3,1/3,1/3), (1/2,2/3,2/3)
cBN	3.6153		F43m	B:(0,0,0),(1/2,1/2,0),(0,1/2,1/2),(1/2,0,1/2) N:(1/4,1/4,1/4),(3/4,3/4,1/4),(1/4,3/4,3/4),(3/4,1/4,3/4)
wBN	2.5505	4.210	$P6_3mc$	B:(0,0,0),(1/3,2/3,1/2) N:(0,03/8),(1/3,2/3,7/8)

Table 2. Lattice parameters, symmetry, and atoms positions for boron nitride phases (Mirkarimi et al., 1997 & Grigoriew & Leceijewicz, 1988).

Boron Nitride (BN) is similar to carbon by forming a hard phase, diamond-like sp^3 bonded phases and soft phase, a graphite-like sp^2 bonded phases). The two equilibrium phases are the hexagonal (h-BN), sp^2 bonded structure, and the cubic (c-BN), sp^3 bonded structure. The hexagonal structure and lattice parameters are similar to the graphite, as rBN, with the exception that the hexagonal layers are arranged directly above each other and rotate 180° between planes in AA'A stacking sequence. Rhombohedral boron nitride is the variant in stacking sequence for a sp^2 bonded phase. The cubic phase for boron consists of tetrahedrally coordinated boron and nitrogen atoms with planes arranged in a three layer stacking sequence (ABCABC). The difference in the stacking sequence for a sp^3 bonded phase produces the wurzitic boron nitride (wBN) with a stacking sequence ABABAB (Mirkarimi et al., 1997).

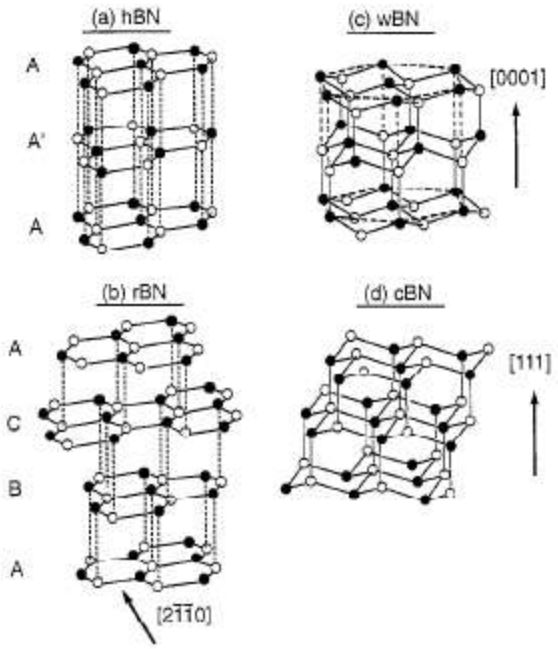

Figure 2. Structure of the sp^3 bonded phases (cBN and wBN) and the sp^2 bonded phases (hBN and rBN) (Mirkarimi et al., 1997).

Cubic boron nitride and wurzitic boron nitride have hard and dense phases which are the product of the sp^3 bond. Another two BN phases are present: turbostratic BN (tBN) and amorphous BN (aBN), which are disordered. The tBN stacking planes are randomly rotated about the c axis. The diffraction patterns produced by tBN are broad and diffuse but can be differentiate from hBn and rBN patterns (Huang & Zhu, 2000).

Hexagonal boron nitride has applications for optical devices in the ultraviolet spectra region and for exciton-based quantum information processing due to its wide bandgap energy of 5.97 eV and large excitation binding energy of 149 meV (Kobayashi et al., 2007). Hexagonal BN is an electrical insulator and thermal conductor. Due to its graphitic phase, it is a good lubricant for reducing wear and friction. Hexagonal BN can be added to other material to produce vibrational damping. Hexagonal BN does not react with oxygen thus can be used in metal machining and as a crucible coating (Ooi, Rajan, Gottlieb, Catherine & Adams, 2006).

The three different BN structures can be produced from rhombohedral boron nitride depending in pressure and temperature conditions. Rhombohedral BN has a similar structure to the hexagonal graphite-like, but with different stacking sequence. Rhombohedral BN is the least study of the BN structures compared to hBN (LeGodec et al., 2000).

Cubic boron nitride was first reported in 1956 to grow as a bulk material, later, in 1970 reports of thin film appeared, but it was not until 1987 that characterization of cubic boron nitride thin films were achieved (Kester, Ailey, & Davis, 1994). Cubic boron nitride is the second material in hardness after diamond (500 Kg/mm^2), it is stable in high temperatures and does not react with ferrous metals, which makes it appropriate for cutting tools, and also can be doped for electronic applications (Kester & Messier, 1992). The cubic phase is stable at high pressure-temperature conditions as reported by Bundy and Wentorf (1962), who developed the phase diagram to demonstrate different crystal structures from hexagonal form. However, recent reports suggest that the cubic phase can be achieved with lower pressures, which determine its stability in ambient conditions (Mirkarimi et al., 1997).

Cubic Boron Nitride Thin Films

Thin films have been used in different electronic and mechanical applications. Within the electronic applications, electronic circuits are of interest due to the reliability aspect especially in the quantum confinement of charges carriers. Thin films are used as surface coating to protect materials at high temperatures such as protective layers in turbine engines. It is also, applied to components subjected to friction and wear due to the contact with other abrasive materials as in knee implants and computer hard disks. Finally, the use of thin films in micro-mechanical systems designed to serve as sensors or actuators show the versatility of thin films applications (Freund & Suresh, 2003).

Cubic boron nitride thin films attracted interest due their properties: second in hardness to diamond with 500 Kg/mm^2, wide band gap (6.4 eV), its ability to be doped with Be (p-type) and Si (n-type), high thermal shock resistance, chemical stability against Fe, stable against oxidation up to 1300^oC , optical transparency and infrared-range make cBN an exceptional material for different applications among the mechanical and electronic areas (Nose et al., 2005; Oechsner, 2006; Abendroth et al., 2004; Deng & Chen, 2006 & K. Sell et al., 2003).

Deposition Methods

The cubic boron nitride depositions achieved by physical vapor deposition (PVD) like ion beam assisted, triode sputtering and r.f. sputtering are the commonly used techniques due the different controllable parameters (Djouadi et al., 2001; Kesler & Messier, 1992 & Ullman et al., 1998). The ion beam assisted techniques use energetic ions from an electric or separate ion beam source. The presence of energetic ion bombardment in the deposition process forces the formation of sp^3 bond, which is needed to form cubic phases. The disadvantage of using ion bombarding is the low purity phase with heavy defect structures and irregular crystallinity (Zhou et al., 2000). Chemical vapor deposition (CVD) methods used to achieve cBN films such as reactive pulsed plasma, micro-wave plasma and r.f. plasma are reported to achieve at least a 80% of cubic boron nitride formation (Zhang, Song & Chen, 1994). However, this process still presents some disadvantages such as the requirements of high vapor pressures of hazardous precursors and gaseous products affecting the substrate material, also, during the process the control of pressures and flow rates may represent defects on the material (Lii, Tsuie & Lee, 2001).

Cubic Boron Nitride Synthesis

The different methods used to deposit BN on silicon substrates have shown a sequence of steps is necessary to reach the cubic structure. First, an amorphous (aBN) layer, which is followed by a textured turbostratic structure or hexagonal, but most of the cases show the tBN formation before the cubic phase. The turbostratic boron nitride as reported by Y.M. Chong et al., 2005, first formed on the substrate and the edges of the (0002) tBN basal planes on the preferential sites that nucleated cBN. However, the role of turbostratic boron nitride is not well understood (Feldermann, Ronning & Hofssas, 2001).

Cubic boron nitride films of 100 nm to 2 μm of thickness had been reported to form by groups such as K. Yamamoto et al., 2000, and S. Ulrich et al., 2006. However, most of techniques used in the deposition process required ion bombardment to form the cubic phase, that introduce high stress in the film and thus causes film delamination (Ulrich et al., 2006). Mirkarimi (1997) observed two factors promoting delamination: compressive stress and water in the ambient environment. Although, achievements of cubic boron nitride films deposited with 20 μm of thickness made by CVD with fluorine chemistry were reported by S. Ulrich, 2006, these are restricted by the substrate material and the necessity of high temperatures up to 1000°C.

The main problem with this field of investigation is the stress caused by the deposition process and the later film delamination. Stress and delamination are reported by Samantaray and Singh (2005) in their cBN synthesis and properties review as the main effects to overcome to achieve high cBN crystalline quality.

CHAPTER III

EXPERIMENTAL PROCEDURE

Sample Preparation

The samples analyzed in chapter IV were deposited by an electron beam evaporation method (PVD) and the procedure described in the work of Nasrazadani and Vemuri, (2004). The electron beam evaporator has four pockets with tungsten crucibles where the material is loaded in the form of rods or pellets. The tungsten crucibles are held at a high potential up to 2kV. A tungsten filament emits electrons at earth potential, and the electrons are accelerated towards the tip of the rod due to the difference in potential. The electron beam induces heat in the material reaching the desire evaporation rate. The ionization of the vapor target measured as ion current is used as an evaporator indicator.

In the previous investigation bulk boron nitrides in pellets were used to achieve the depositions. The pellets were loaded in the crucibles, which were heated by high current applied to the filament, reached 2000^{o}C and started to evaporate the material. The vaporized material was deposited on a silicon wafer (100) heated to temperatures as high as 400^{o}C. A filament current vs time plot indicated the process duration which was around 65 minutes. An Oxford Applied Research (OAR) HPEB4 with Coolflow Refrigerated Recirculator CFT-33 was used in the deposition process with the following general characteristics.

Table 3. Deposition parameters for BN depositions. (Nasrazadani & Vemuri, 2005).

Section	**Conditions**
Chamber pressure	$4x10^{-7}$ Torr
Operating pressure	$3x10^{-5}$ Torr
Substrate temperature	400^{o}C

Filament temperature	$2000^{o}C$
Electron beam energy	2kV
Source to target distance	50 mm
Filament current	4 Amps

Boron nitride was deposited on Silicon wafers (100) of 45 mm radius and 1mm thickness, which were cleaned using HF acid. The cleanness of the Silicon wafer was a main factor for the achievement of stable and smooth films.

Thin Films Characterization Techniques

The characterization techniques used in this research for thin films are Fourier Transform Infrared Spectrophotometry (FTIR), Scanning Electron Microscopy (SEM), X-Ray Spectroscopy (XRD), Transmission Electron Microscopy (TEM), and Atomic Force Microscopy (AFM).

Fourier Transform Infrared Spectroscopy (FTIR).

Fourier transform infrared spectrophotometry (FTIR) is a nondestructive technique for solid and thin films used for quantitative analyses. Infrared spectrophotometry provides information about the chemical bonding that varies depending on the material upon investigation. In this investigation a Nicolet Aviator 370 DTGS FTIR in Attenuated Total Reflection (ATR) mode with Omnic software was used to obtain infrared spectra in transmittance or absorbance vs wavelength.

Operation. A beam of light travels through the sample with I_o intensity and leaves the sample with I_t intensity that interacted with the different bonds in the sample. The ratio of these intensities as a function of the frequency of the light is the infrared spectrum, which is represented by:

$$T_w = \left(\frac{I_t}{I_o} \right)_w$$

where T_w is the transmittance of the sample. If the case is light reflected from the surface is measured, then the ratio is the reflectance of the spectrum. The beam is reflected through an optically dense crystal at a certain angle. Once the sample is placed in contact with the crystal, the infrared radiation interacts with the sample producing a transmittance-like spectrum. At the surface of the sample an evanescent wave is produced. The energy produced from the evanescent wave that is altered or attenuated passes back to the beam (Figure 3) which exits at the end of the crystal to form the spectrum, as is show in Figure 3.

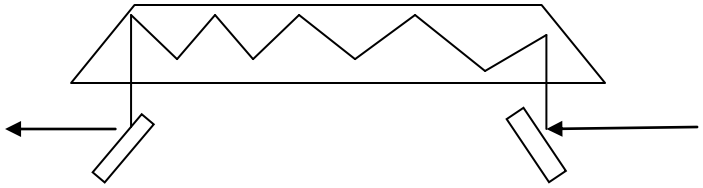

Figure 3. Schematic of Attenuated Total Reflection (ATR) in FTIR.

The infrared spectrum has three characteristics that could be used to make quantitative analyses: peak position, integrated peak intensity and peak width. The peak position is the most used for qualitative identification due the unique chemical groups characteristics. The integrated peak intensity is proportional to the concentration of absorbing bonds, when a band arises from a particular vibrational mode. The peak width is a function of the homogeneity of the chemical bonding, where the full width at half maximum (FWHM) is a characteristic for defects and bond strain. The change in strength of chemical bonds cause shifts in peak position (Brundle, Evans & Wilson, 1992).

Scanning Electron Microscopy (SEM).

SEM is the most common instrument when it comes to deal with high resolution and material characterization especially for surface images of thin films. The image obtained from a sample is magnified to the point that is similar to a traditional microscope but with more depth of field, making this technique useful for morphological analysis. For this investigation an FEI Quanta 200 ESEM, which is an environmental scanning electron microscope, was used to characterize surface features and examine depositions.

Operation. The principle of operation of a SEM starts with an electron gun that produces a beam of electrons, which is accelerated towards the sample to be rastered. The beam of electrons passes through one or two condenser lenses forming a fine probe that later is rastered over the sample by the scanning coils in the objective lens (Figure 4). The electrons penetrate the surface forming a tear drop volume that creates the scattering effect which is the emission of electrons or photons. These electrons or photons are collected by detectors corresponding to each type of scattered electrons or photons. There are three types of images: secondary electrons images, backscattered electrons images and elemental X-rays. The electrons detected are converted into voltages and amplified and then applied to the cold cathode tube (CRT) grid to produce the image. The electron beam raster over the surface creates for each point of the sample a point in the image (Brundle et al., 1992).

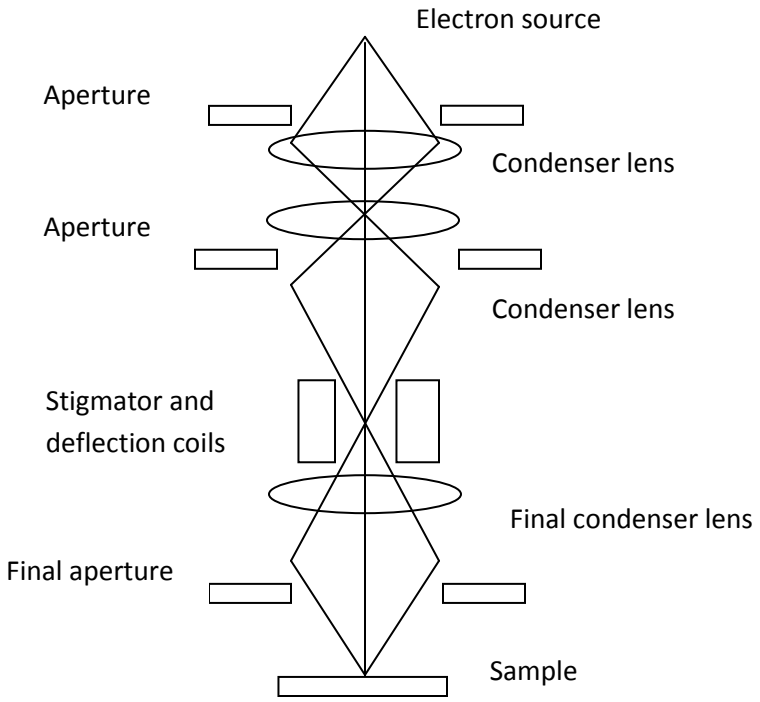

Figure 4. Schematic of Scanning Electron Microscope.

Energy dispersive X-ray spectroscopy (EDS).

Energy dispersive X-ray spectroscopy is widely used for chemical characterization. Each element in the periodic table has a unique electronic configuration and thus gives a specific (X-ray) response to high energy radiation, which allows easy recognition of deposited elements. For this investigation the Quanta 200 equipped with EDAX was used to perform the chemical analyses on the samples' surfaces.

Operation. Most SEM and TEM microscopes are equipped with EDS. The ionization of atoms takes place by a knocked electron from an inner shell. The ion to go back its ground state by an electron from a higher energy outer shell that fills the vacant inner shell energies. In this process, electrons release an amount of energy equal to the difference between shells. This energy is unique for each atomic transition, which is represented as X-ray photons or Auger

electrons as shown in Figure 5. The process of filling the shells can continue until it reaches all the atomic levels that result in many emissions.

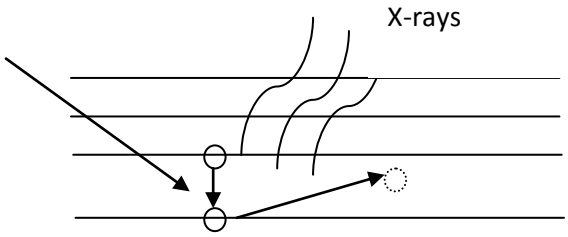

Figure 5. Electron filling the next energy level and X-ray

X-ray diffraction (XRD).

The X-ray diffraction is a non-destructive technique used to characterize crystalline phases and measure structural properties such as strain state, grain size, epitaxy, preferred orientation and defect structure. XRD is used with thin films to measure atomic spacing and strain states. The intensities measured by XRD are sensitive to the atomic number (Z) of the elements, which can be high with high Z elements while the intensity is low with low Z elements thus the sensitivity depend on the element atomic weight. In this investigation a Rigaku Ultima III X-ray Diffractometer was used in a symmetric mode to obtain the diffraction intensities of the boron nitride samples and characterized their crystal structure. A JCPDS library was used to identify element diffractions.

Operation. In this system a collimated beam of X-rays with a wavelength λ approximately of 0.5 to 2 Å is used. The beam is incident on the specimen and is diffracted by the crystals phases describe by Bragg's law:

$$\lambda = 2d \sin\theta$$

where d is distance between planes in the crystalline phase, θ is the angle between the atomic planes and the incident beam and λ is wavelength of the incident and reflected beam.

The intensity obtained in the spectrum is the difference between the diffraction angle 2θ and the sample orientation, with peaks when a constructive interference from x-rays scattered by the atomic planes in crystal (C.R. Richard et al., 1992). The scattering is demostrated in Figure 6 .

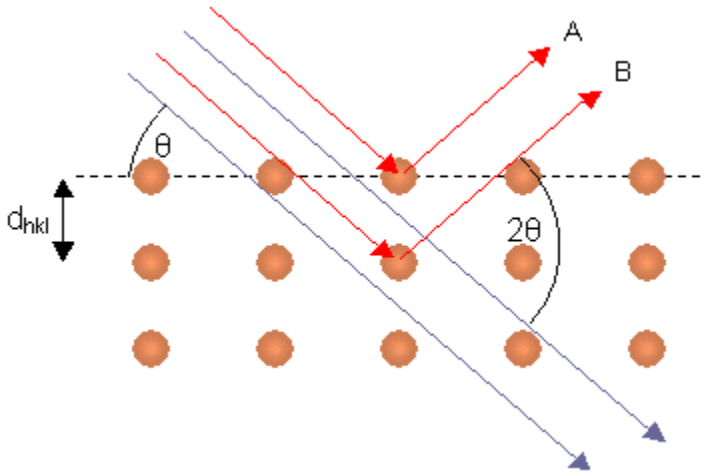

Figure 6. Representation of Bragg's law (http://www.doitpoms.ac.uk/tlplib/xray-diffraction/bragg.php).

Transmission Electron Microscopy (TEM).

The capability of the transmission electron microscopy (TEM) to provide a high image resolution and diffraction patterns makes it a standard technique for characterization of thin films. Although the process to get a *good* sample can be tedious and difficult the in-depth information about crystal lattice, phase identification, grain size, and composition within the material is worthy the sample preparation (Samantaray et al., 2005).

Sample preparation can be achieved manually or using Focused Ion Beam (FIB). The manual method has series of steps to get a good sample. For this investigation, a cross sectional process was required to achieve characterization with the TEM. The manual sample preparation starts by gluing a set of samples with each other, face to face, to have more area to be analyzed. Then this brick of packed samples is sliced as thin as possible and is subsequently milled and polished. The last two steps are grinding and ion milling. Throughout the entire process experience plays

an important role due to the sample fragility. More than ten sample preparations were conducted to obtain one good sample to be analyzed with TEM. The number of samples and time to get one good sample must be considered for this type of sample preparation.

The FIB alternative for sample preparation saves time and samples, but doesn't secure a good sample image. The FIB process called lift-out can be describe as cut of a rectangular volume, lifted by a needle and then placed on a grid. Samples are milled to get to appropriate thickness for TEM, which is less than 100 nm. The process in the FIB requires three hours to prepare a sample, which when compared with the manual method, saves research time; but the FIB manipulation require months of training.

In this investigation a Philips EM420 with Selected Area Diffraction (SAD) and convergent beam electron diffraction mode (CBED) diffraction capabilities and FEA Nova 200 Dual Beam FIB/FEGSEM was used to obtain resourceful data to be analyzed in chapter IV.

Operation. A focused electron beam is applied to a thin film which produces scattered and unscattered electrons. The electron beam is focused by a series of lenses (illumination system) before and after the sample, to deliver the signal to the detector, which is a fluorescent screen, a film plate or a video camera. The magnification achieved by the TEM is product of the small wavelength of the electrons and the scattering electrons form a picture or a diffraction pattern (Richard et al.,1992).

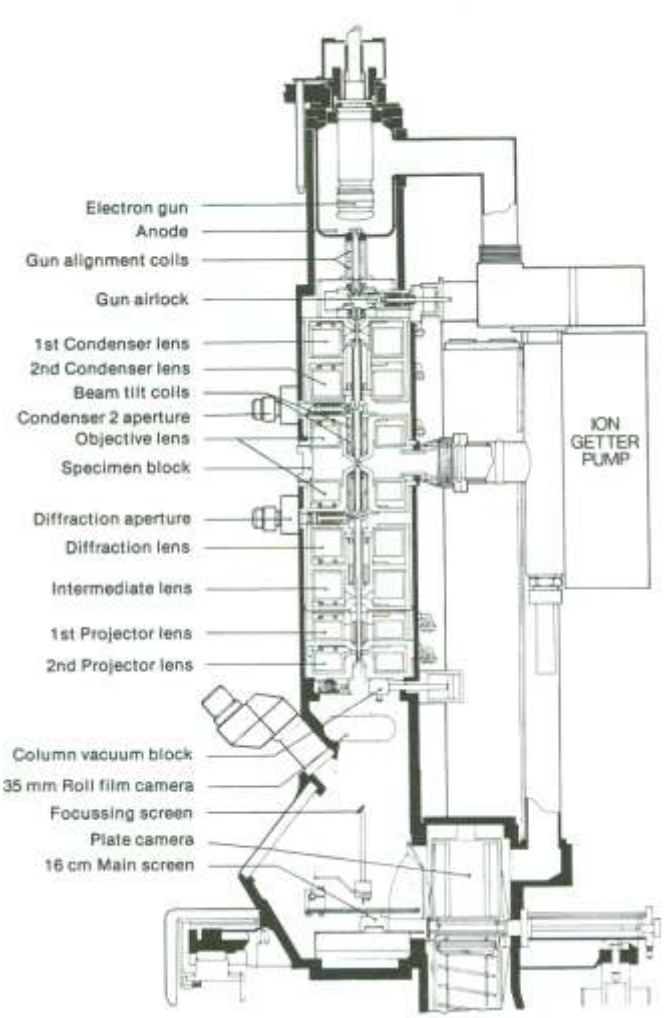

Figure 7. Schematic of Transmission Electron Microscope column. (Brundle et at., 1992)

Atomic Force Microscopy (AFM).

Atomic Force Microscopy (AFM) is among most common scanning probe techniques. It is a technique that produces a real-life imaging with a topographic surface image. The AFM device has an atomic resolution in the x, y and z directions. AFM can be used to manipulate atoms and structures on different surfaces. A cantilever with a sharp tip is used to scan the surface creating the map of the surface. For this investigation a Multimode Scanning Probe Microscope with Nanocospe III Digital Instrument software was used to obtain the surfaces images (Brundle et al., 1992).

Operation. In this type of scanning, a sharp tip mounted on a flexible cantilever produces the image. The tip approaches the surface and within a few Å the van der Waals force between the atoms, in the sharp tip and the atoms in the surface occurs, causes a deflection of the cantilever. The interaction forces indicate the different features of the surface which are a function of the distance between the tip and the sample. The cantilever deflection response has to be measured accurately by an optical-lever or beam-bounce detection system. Light from a laser diode is reflected from the back of the cantilever to a position-sensitive photodiode describing a position by the cantilever transformed into a specific position by the photodiode. A common cantilever is 100-200 µm and 0.6 µm thick with a sharp tip with a radius of about 400 Å. The cantilever is coated with gold to improve reflectance (Brundle et al., 1992).

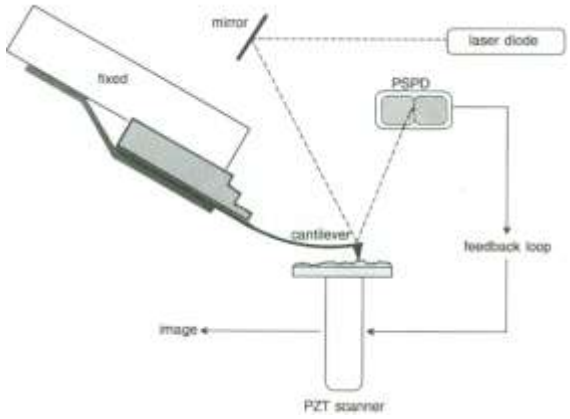

Figure 8. Schematic of Atomic Force Microscopy. (Brundle et al., 1992)

Tribometer

A tribometer measures friction. Friction is the resistance of a solid body to motion during sliding or rolling. Friction tests are conducted to select a material for a specific operation in most of the cases. The information obtained from the material properties are important for future applications. Thin films properties as adhesion and hardness can be measured from this type of test (B. Bhushan, 2002). For this investigation a Pin on Disk machine configuration, ISC-200

Tribometer, was used to measured friction from the film. The friction coefficients were obtained by applying two loads, 100 g and 50 g, with constant velocity at 1.64 cm/s.

Operation. The Pin on Disk machines consist of a spherical end pin (steel ball) loaded against the sample. The sample is placed over a rotating flat disk. The load is pressed against the sample by a lever and weights. The rpm or linear velocity and the number of cycles are set. Most of the measurement parameters are standardized.

Figure 9. ISC-200 Tribometer

CHAPTER IV

RESULTS AND DISCUSSIONS

Introduction

Cubic boron nitride films have significant industrial potential due to their properties. Cubic boron nitride (cBN) with a hardness of about 5000 kg/mm is second only to diamond. cBN films do not react with ferrous metals, have electronic wide band gap and good thermal conductivity all of which makes cBN a good candidate for tooling and electronic applications.

The characterization of BN films has been done since 1988 with different techniques. The work from Mirkarimi et al., (1997) and Samantaray et al., (2006) present a review of BN synthesis and characterization. Fourier Transform Infrared Spectroscopy (FTIR), X-ray diffraction (XRD) and Transmission Electron Microscopy (TEM) are characterization techniques that are commonly used to analyze BN films. Table 4 shows characterization wavenumbers of polymorphs of BN.

Table 4. FTIR wavenumbers for BN films.

Boron nitride polymorphs	**Wavenumbers (cm^{-1})**
cBN	1050,1340
wBN	1090,1120,1230
hBN	783,828,1400
rBN	Not available

The wavenumber at 1050 cm^{-1} is one of the main characteristics to identify cBN formation in the sample. The growth of cubic phase, as reported in the literature (Chong et al., 2005 and Feldermann et al., 2001), is by stages. The first stage is the nucleation of a hexagonal

phase that also can be turbostratic. The IR spectra of hexagonal BN phase show two peaks at 790 and 1400 cm^{-1} that can be interpreted as a good sign for the deposition development. A general FTIR spectrum with the different phases is presented in Figure 10.

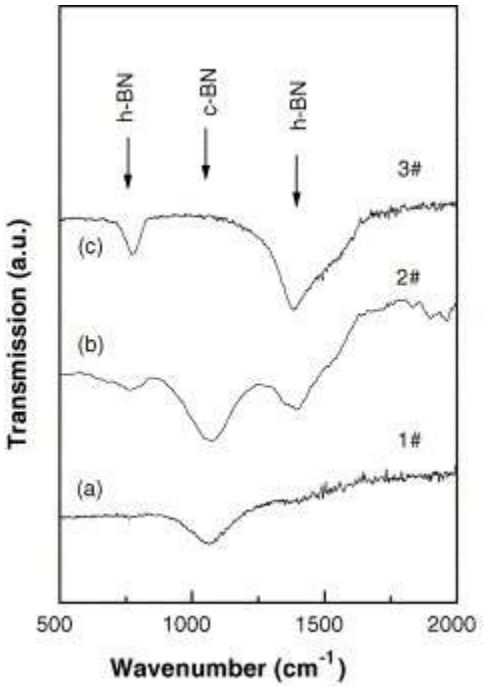

Figure 10. FTIR spectra of different BN phases. (Deng & Chen et al., 2006)

X-ray diffraction is a nondestructive characterization method which is used to identify crystalline structures. The diffraction patterns from BN films with X-ray and electrons are similar in principle. Electron diffraction has better counting statistics and is thus more reliable for thin films studies. The theoretical values for interplanar spacing are given in Table 5. Based on the d-spacing and Bragg's law, the diffraction angles are obtained, groups like Ulrich et al. (2005) and Tian, Pan, He & Xu (2000) reported characteristic angles to identify BN phases. Diffraction spectra in Figure 11 from the work of J. Yu et al. (2005) show the diffraction from cBN and silicon as-deposited and annealed films.

Table 5. Lattice plane spacing and diffraction angle for major of boron nitride phases.

Plane (d) spacing (nm)	**Structure & (hkl)**	**Diffraction angle (2θ)**
0.333	hBN (0002)	26°
0.209	cBN(111)	43°
0.181	cBN(200)	50°
0.128	cBN(220)	74°
0.109	cBN(311)	90°
0.090	cBN(400)	118°
0.083	cBN(331)	137°

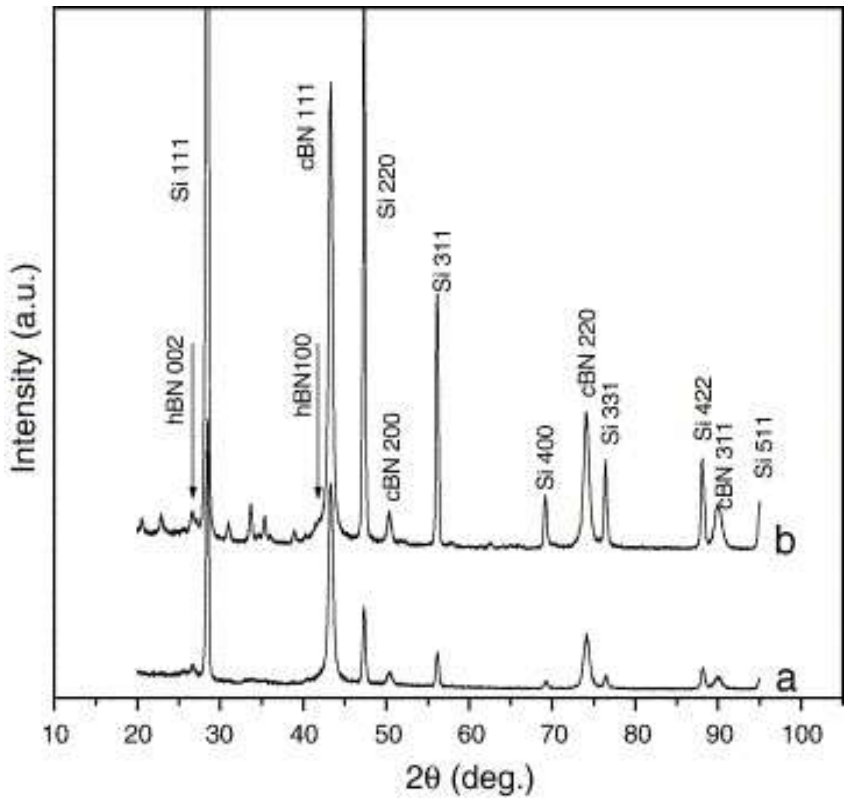

Figure 11. XRD patterns of the as-deposited (a) and annealed (b) of cBN films (Yu et al., 2005)

Electron diffraction is obtained by selecting an area that is has no distortion. The selected area diffraction (SAD) is the result of constructive wave interference that satisfies Bragg's law. Electron diffraction is used more frequently due the advantages of obtaining information from the bulk of the material rather than the surface. Specific patterns from this characterization are described in works of Mirkarimi et al. (1997) and Latteman et al. (2005), among others. Figure 12 depicts a BN electron diffraction pattern from Latterman et al. (2005).

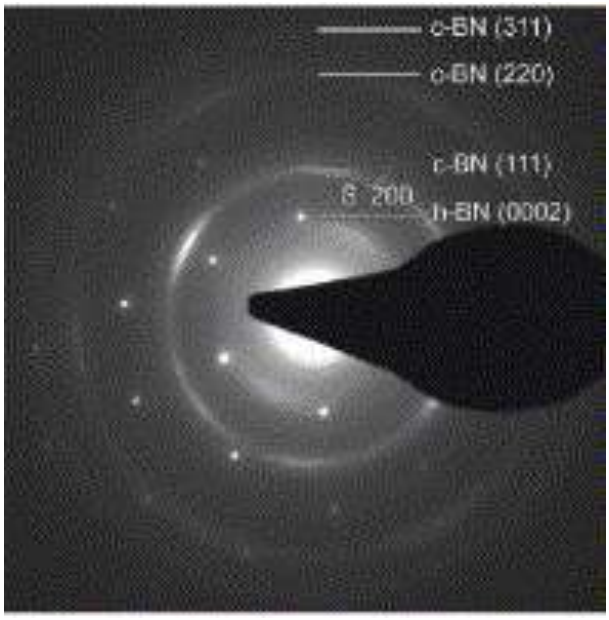

Figure 12. Diffraction pattern from a boron nitride film. (Latterman et al., 2005)

Samples Characterized

The ten samples listed in Table 6 analyzed in this chapter varied in deposition time from ½ to 2 hours and deposition temperatures from room temperature to 400°C. The time and temperature were varied to enhance phase formation according with the work of Gimeno, Munoz & Lousa (1996), and Zhou et al.(2002).

Table 6. Deposition parameters used in BN formation.

Sample No	**Conditions (temperature-time)**
1	Room temperature- ½ hour
2	Room temperature- ½ hour
3	Room temperature- ½ hour
4	Room temperature-1 hour
5	400^{o}C- ½ hour
6	400^{o}C- ½ hour

7	400^{o}C- ½ hour
8	400^{o}C-1 hour
9	400^{o}C- 1 hour
10	400^{o}C- 2 hour

Characterization with FTIR, and XRD were made to all samples, which give qualitative analyses of the boron nitride depositions. The XRD and TEM were used to determine the phase formation. AFM was also used to measure thickness and the root mean square (rms) surface roughness. These techniques are nondestructive and there is minimal sample preparations involved.

In the cases where the deposition time and temperature were increased, the characterization with TEM and AFM were used to measured thickness, topography and crystal structure identification. A sample deposited for two hours at 400°C was friction tested. Samples are analyzed in sequential order as given in Table 6.

Samples deposited for ½ hour at room temperature.

Sample 1, 2 and 3 were deposited for ½ hour at room temperature. Samples deposition conditions are described in Table 7.

Table 7. Deposition conditions of samples 1, 2 and 3.

Parameter	**Value**
Initial pressure	4.3X10^{-7} torr
Working pressure	2.6X10^{-3} torr
Filament current	4 amps
Emission current	53 mA

Deposition time	½ hour
Cooling water supply	20^{o}C
Substrate temperature	Room temperature

The FTIR spectra, Figure 13 (a-c), show transmittance bonds around 940 cm^{-1} and 1224 cm^{-1} with low intensities, which are representatives of hBN (Kester et al., 1994). The 1050 cm^{-1} peak which is indicative of cBN not being present in the spectra for samples deposited for ½ hour at room temperature. Therefore no cubic phase formed on these samples. Literature data suggest cBN deposition needs higher substrate temperatures and hBN formation is more feasible under these conditions.

Samples deposited for ½ hour at room temperature show SiO_2 infrared characteristics bond at 1050 cm^{-1} and a shoulder at 1125 cm^{-1} wavenumbers, which help to differentiate cBN structure from SiO_2. Mirkarimi et al.1997, reports that cBN wavenumbers can be confused with SiO_2 showing a bond between about 1100 and 1050 cm^{-1}. The SiO_2 feature has a shoulder at about 1150 cm^{-1} helping to differentiate the cBN from the oxide.

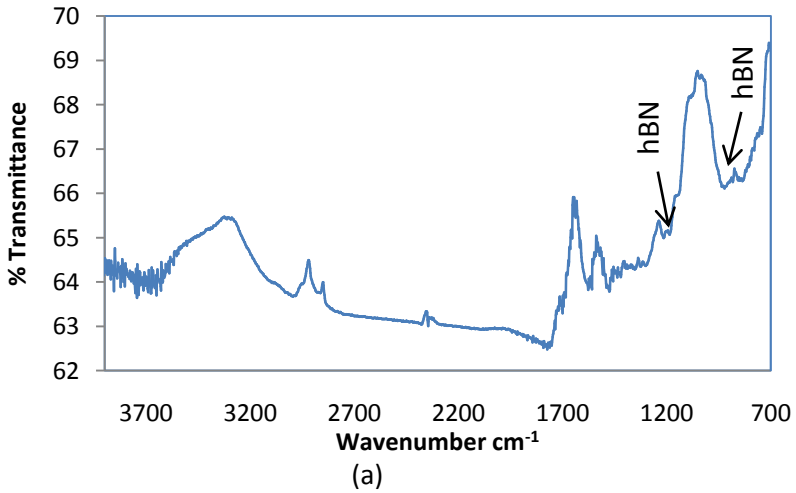

(a)

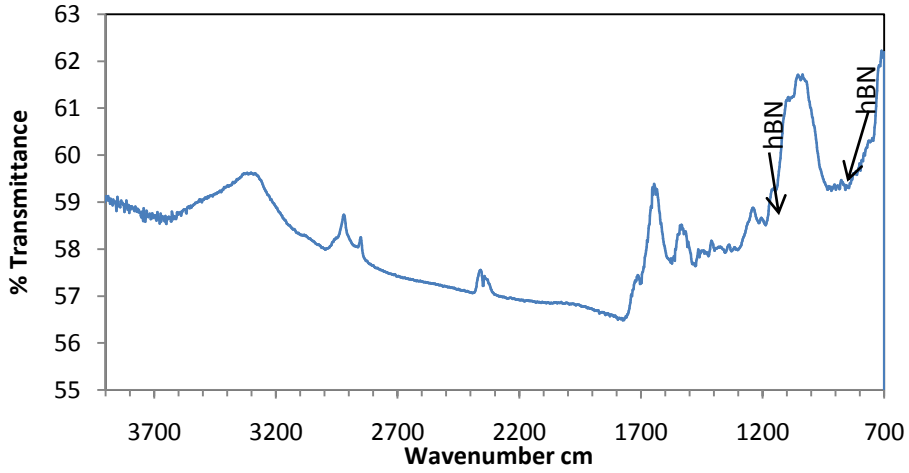

(b)

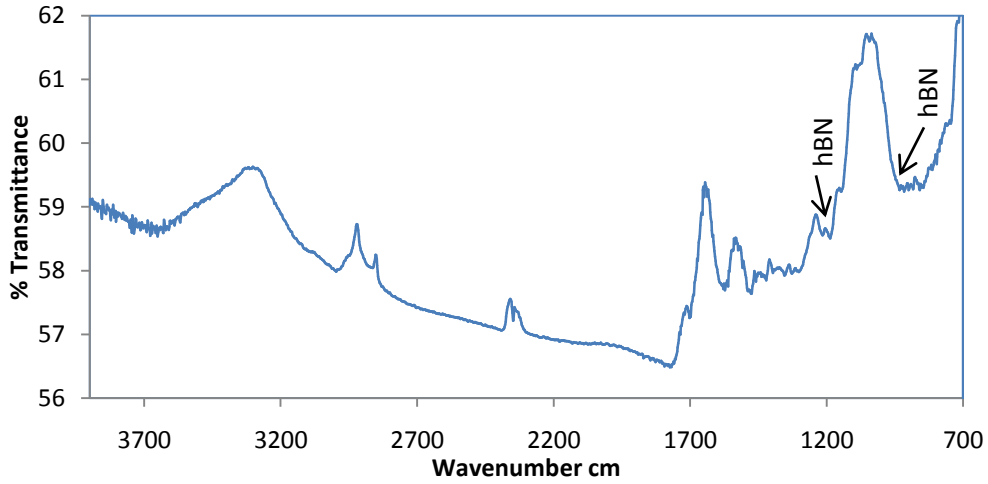

(c)

Figure 13. FTIR spectra of sample 1 (a), sample 2 (b) and sample 3 (c) deposited for ½ hour at room temperature

The XRD, Figure 14, shows high intensity peaks at 70° (2θ) corresponding to Si (400). According with Figure 14, there is no diffraction from the BN film deposited. Cubic phase from BN has a significant diffraction at 43° that is a (111) orientation, which is not present in this deposition. The hexagonal phase is not present due the thickness of the layer. Figure 14 shows a SiO_2 diffraction angle with low intensity. SiO_2 could have been caused by the exposure of the substrate to the environment.

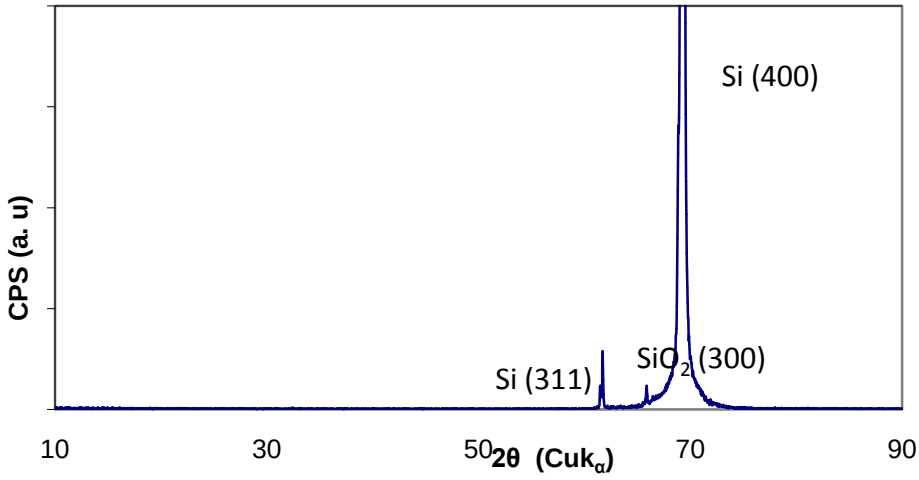
Si (400)
CPS (a. u)
Si (311)
SiO2 (300)
10
30
50
70
90
2θ (Cukα)

(a)

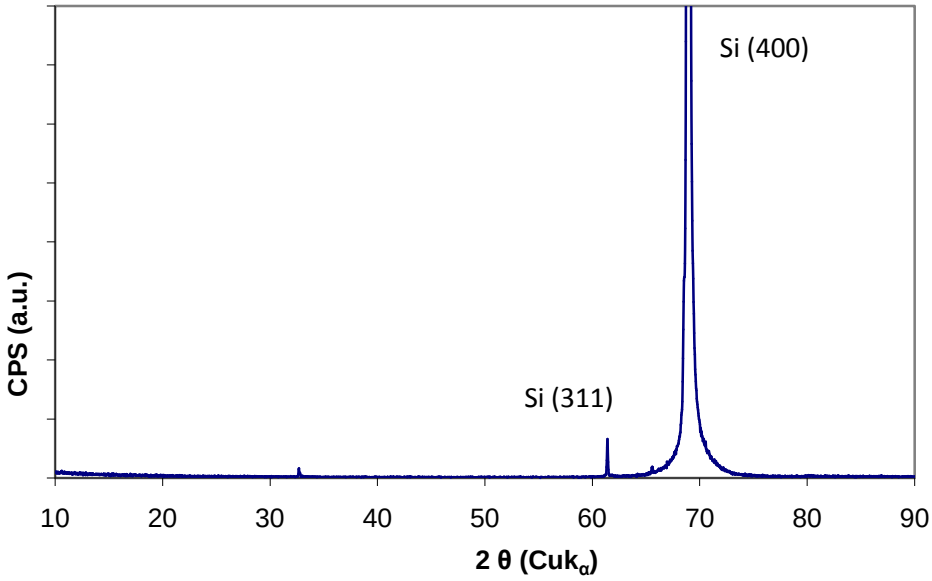
Si (400)
CPS (a.u.)
Si (311)
10
20
30
40
50
60
70
80
90
2 θ (Cukα)

(b)

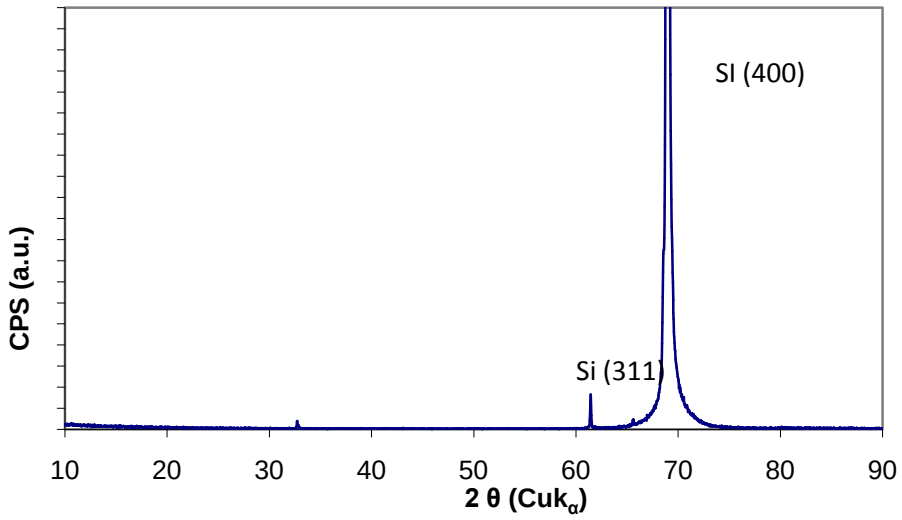

(c)

Figure 14. XRD spectra of sample 1 (a), sample 2 (b) and sample 3 (c) deposited for ½ hour at room temperature

Figure 15 (a-c) represent the SEM images from samples deposited for ½ hour at room temperature. Figure 15 (a) and (b) show no specific film characteristics. The particles over the surfaces are possible contaminants from the handling of the samples. Figure 15 (c) depicts porous formation at different spots that could be assumed as a nonuniform layer. Figure 15 (d) shows a EDS from sample 3. An emission at 0.185 keV from the principal emission of boron in present in the EDS spectrum. Nitrogen is present with low counts. Nitrogen has a principal emission at 0.392 keV and Silicon has emission at 1.70 KeV. Oxygen and carbon have the peaks with higher counts in the spectrum.

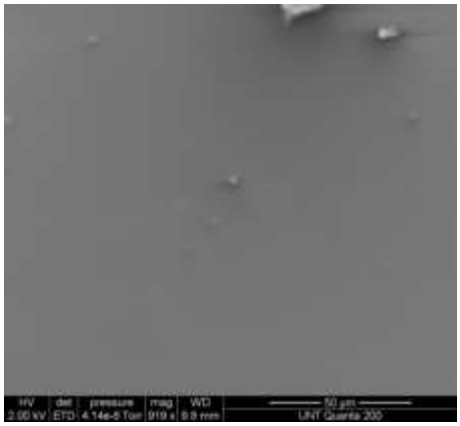

(a)

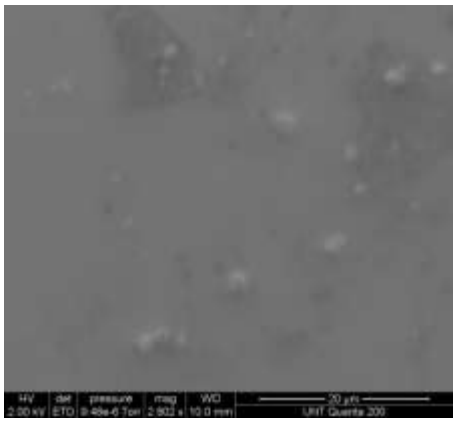

(b)

(c)

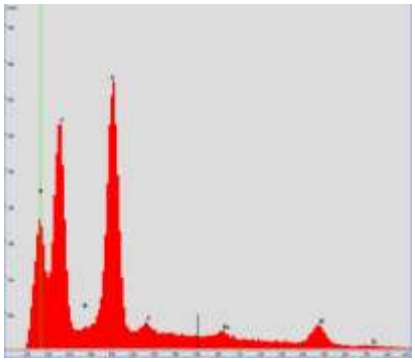

(d)

Figure 15. SEM images for sample 1 (a), sample 2 (b), sample 3 (c) and EDS spectrum from sample 3 (d) with 2 kV.

Sample deposited for 1 hour at room temperature.

Sample 4 was exposed for 1 hour at room temperature. Based on the literature the deposition time is one of the factors that control the quality of cBN depositions (Oechsner, 2006). The deposition paramaters are described in Table 8.

Table 8. Deposition parameters for sample deposited for 1 hour at room temperature.

Parameter	**Value**
Initial pressure	$4.8X10^{-7}$ torr
Woking pressure	$3.9X10^{-5}$ torr
Filament current	4 amps
Emission current	54 mA
Deposition time	1 hour
Cooling water supply	$20^{o}C$
Substrate temperature	Room temperature

Figure 16 (a) shows an infrared spectrum hexagonal phase with wavenumbers around 1110 cm^{-1} and 900 cm^{-1} . The characteristic of hexagonal formation is present according with literature (Mirkirami et al., 1997; Deng & Chen, 2006 & Samantaray et al., 2005). The infrared spectrum of depositions for 1 hour at room temperature indicate the presence of hexagonal phase of boron nitride along with small fraction of cubic phase. The absortion bond at 1060 cm^{-1} wavenumber is a characteristic signal of cubic formation. Though the peak intensity is low, cubic phase has formed after the formation of a hexagonal layer.

The XRD sepctrum, Figure 16 (b), shows three distinct peaks. The Si (100) has high intensity due the substrate material. The hBN intensity is a clear sign that boron nitride hexagonal phase had developed over the the substrate surface. The hBN formation is the first stage to growth of cBN as reported in the literature (Chong et al., 2006). The next peak is a cubic boron nitride which is a characteristic (111) diffraction. The cBN (111) is frequently reported as the main factor for cBN thin films characterization. The intensity of this peak is too low to

assume that the deposition was uniform. The deposition time for one hour had influenced the phase growth in sample 4.

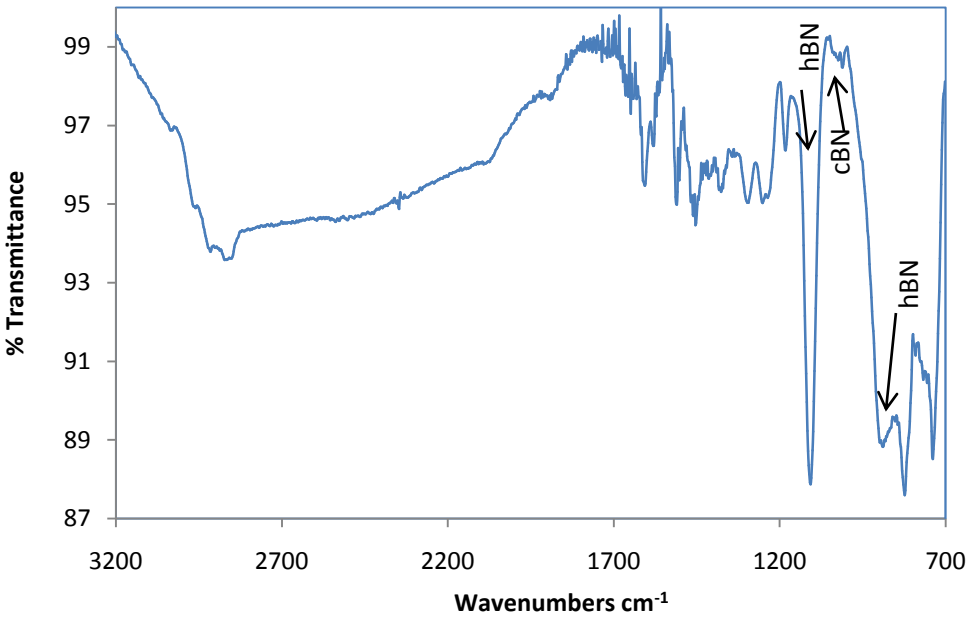

(a)

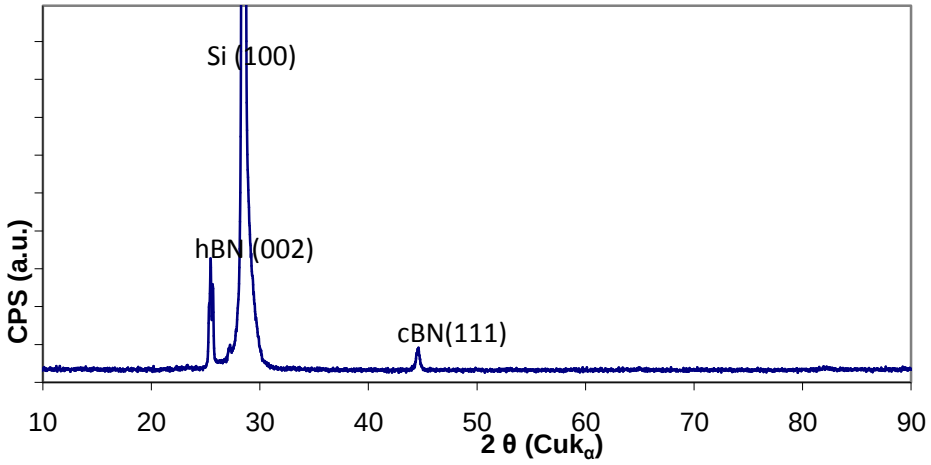

(b)

Figure 16. FTIR spectrum (a) and XRD pattern (b) for a sample deposited for 1 hour at room temperature

Figure 17 is an image obtained with SEM with a 2817X magnification. The image depicts the film deposited over the surface. The layer formation is depicted in the image with a

uniform deposition that could be assumed as a hexagonal phase based in the FTIR and XRD spectra.

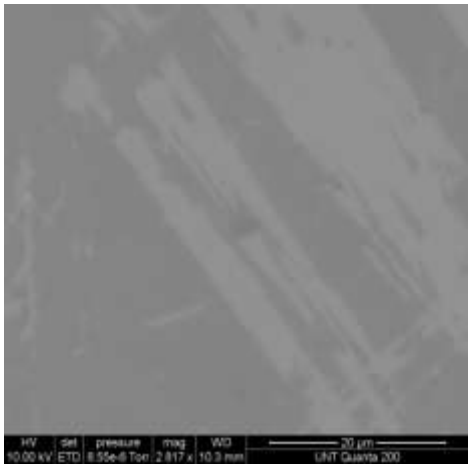

Figure 17. SEM image for a sample deposited for 1 hour at room temperature

.

TEM samples were prepared by lift-out process described in chapter III. The image obtained using a Philips EM420 is the cross section for sample 4 deposited for ½ hour at room temperature at 3400X magnification. Figure 18 exposes the silicon substrate and the platimun used to obtained the cross section on top of the depositon. The BN film is clearly in the middle of both. The thickness was measured with ImageJ software. The thickness is 15 nm for a sample with 1 hour deposition at room temperature.

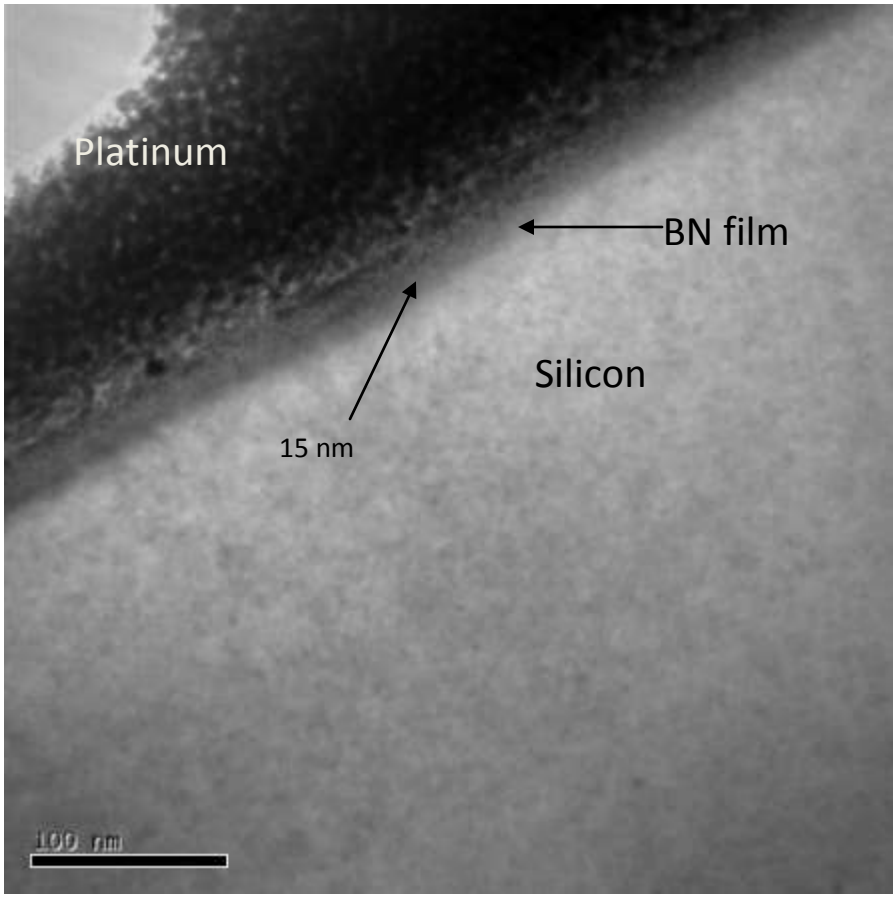

Figure 18. TEM image from sample deposited for 1 hour at room temperature.

Figure 19 (a) is silicon diffraction obtained with the Philips 420EM using a 165 camera length. Figure 19 (b) is the diffraction of an amorphous platinum with a 139 pm radius. With a film thickeness near to 15 nm, diffraction patterns are difficult to obtain due to the spot size. The diffraction from the silicon and platimun are used as a reference to differentiate BN film diffraction patterns.

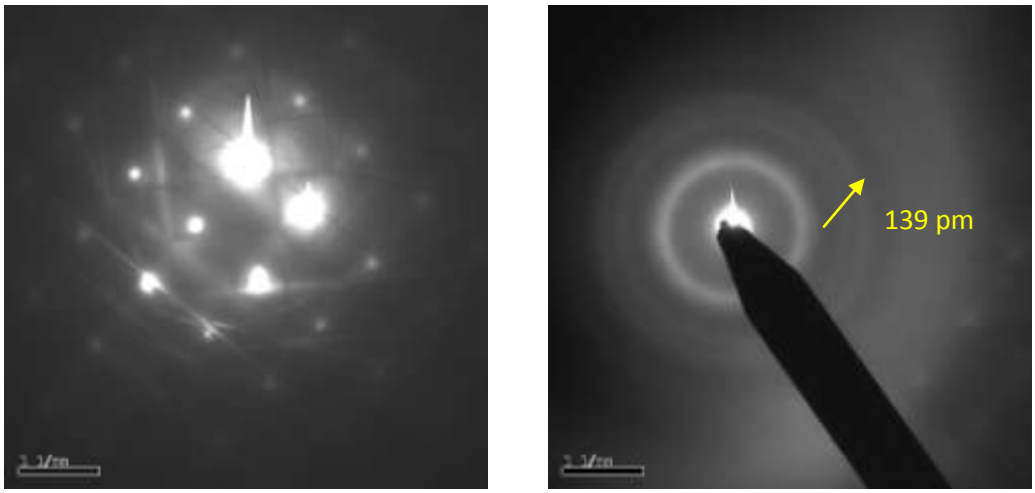

(a) **(b)**

Figure 19. Silicon diffraction (a) and amorphous platinum diffraction (b) from sample 4 with 165 camera length.

The diffraction in Figure 20 was captured from the film. The thickness of the BN film is smaller than the spot size of the beam used in the TEM thus obtaining diffraction patterns from the BN film is difficult. The silicon structure is clear in the image. The amorphous ring from Pt is also present, but, as expected, the diffraction is not strong (Figure 19 b).

The brightest ring in Figure 20 has 0.1802 nm for lattice plane spacing. This value is close to the theorical value 0.181 nm for cBN (200). The presence of cBN (200) diffraction demonstrated that as the deposition time increased cubic phase formed on top of hBN phase. The hexagonal ring is close to the indicator making it difficult to differentiate from the beam.

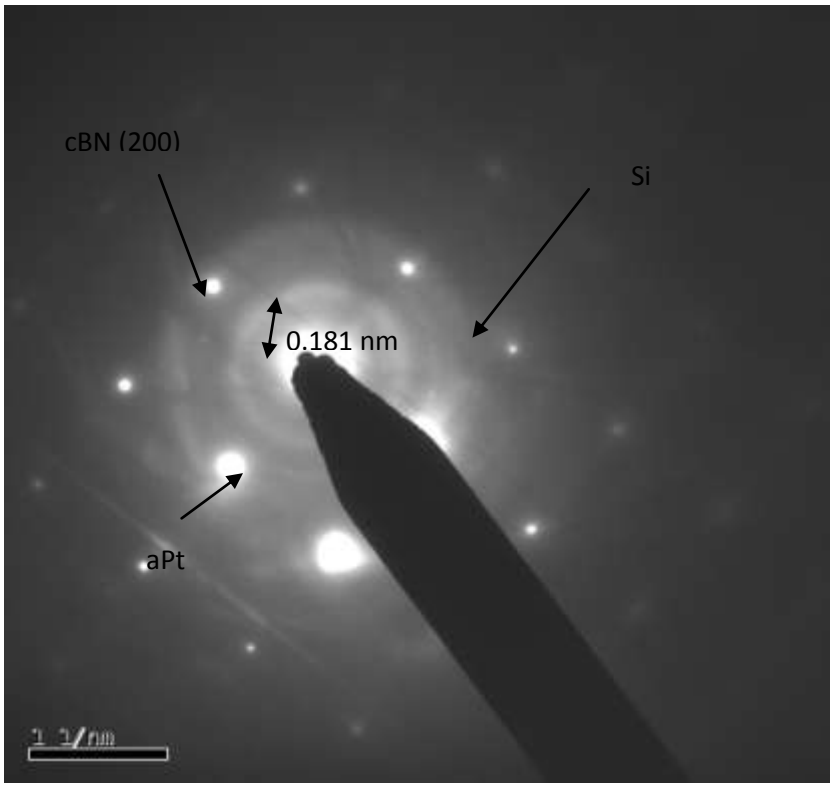

Figure 20. TEM SAD diffraction from BN film.

Samples deposited for ½ hour at 400°C.

Samples were deposited for ½ hour at 400^{o}C. Deposition time was reduced and temperature increased to determine if the temperature influences the growth of the cubic phase. The parameters for sample 5, 6 and 7 are described in Table 9. Samples were characterized with FTIR and XRD techniques to determine phase formation.

Table 9. Deposition parameters for sample 5, 6 and 7 for ½ hour at 400°C.

Deposition parameters	**Value**
Initial pressure	$4X10^{-7}$ torr
Working pressure	$3.8X10^{-5}$ torr
Filament current	4 amps
Emission current	54 mA

Deposition time	½ hour
Cooling supply water	20^{o}C
Substrate temperature	400^{o}C

Samples deposited for ½ hour at 400°C, Figure 21 (a-c), show hexagonal formation as indicated by the wavenumbers 960 cm^{-1} and 1120 cm^{-1} (D. J. Kester et al., 1994). The deposition time for samples 5, 6 and 7 is enough to form hexagonal layers as the first stage for cubic phase. Though there is hexagonal phase in the infrared spectrums, it is not consistent to reach a cubic phase.

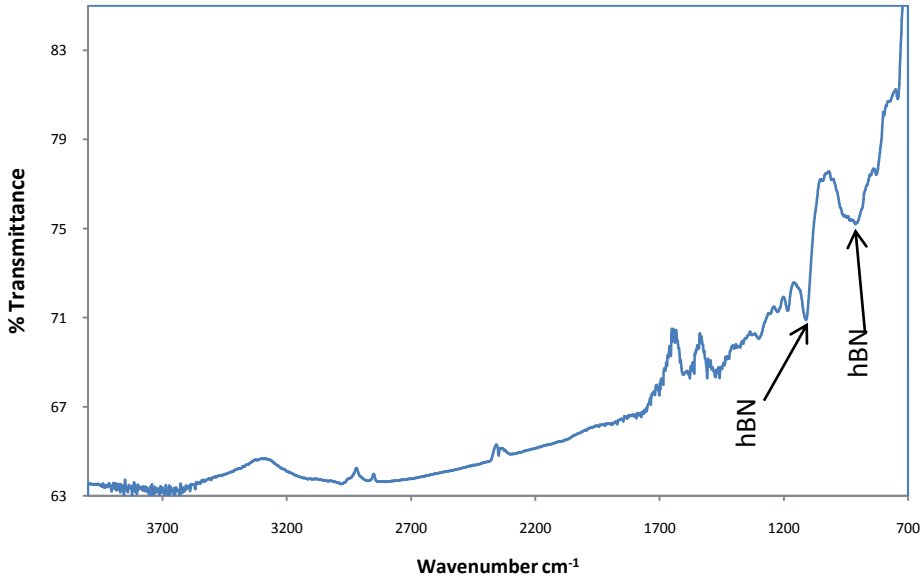

(a)

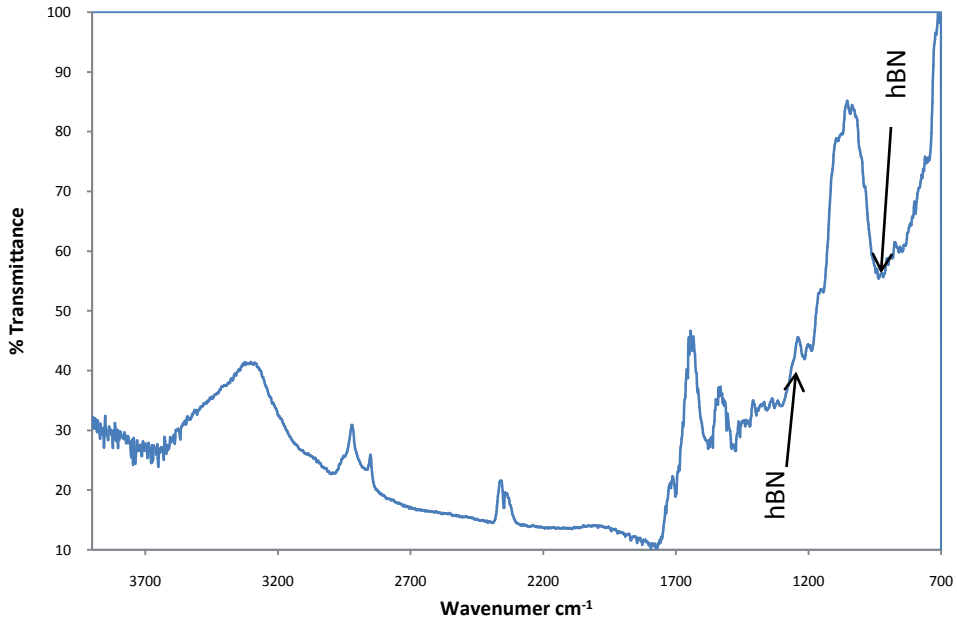

(b)

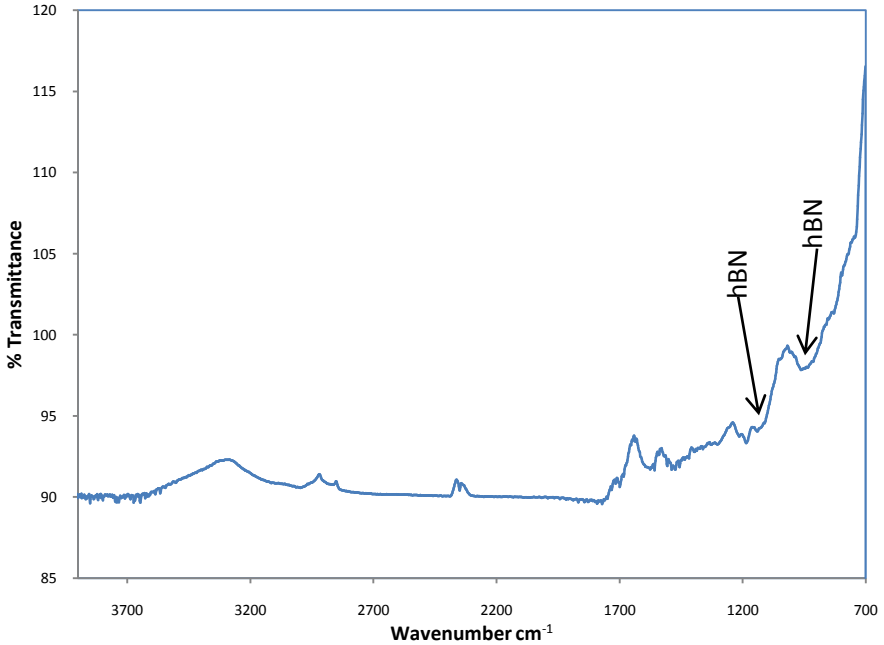

(c)

Figure 21. FTIR spectra of sample 5 (a), sample 6 (b) sample 7 (c) deposited for ½ hour at 400°C.

XRD characterization done on samples deposited for ½ hour at room temperature show no hexagonal nor cubic phase formed. There are no diffractions from BN depositions. XRD and FTIR demonstrate that the deposition time is not enough to form a hexagonal uniform layer. SEM images, Figure 22 (a-c), show no formation of BN phases on the substrate. Samples for hour at 400°C did not show any phase growth. SEM images with FTIR and XRD spectra demostrate that the deposition time had to be increased.

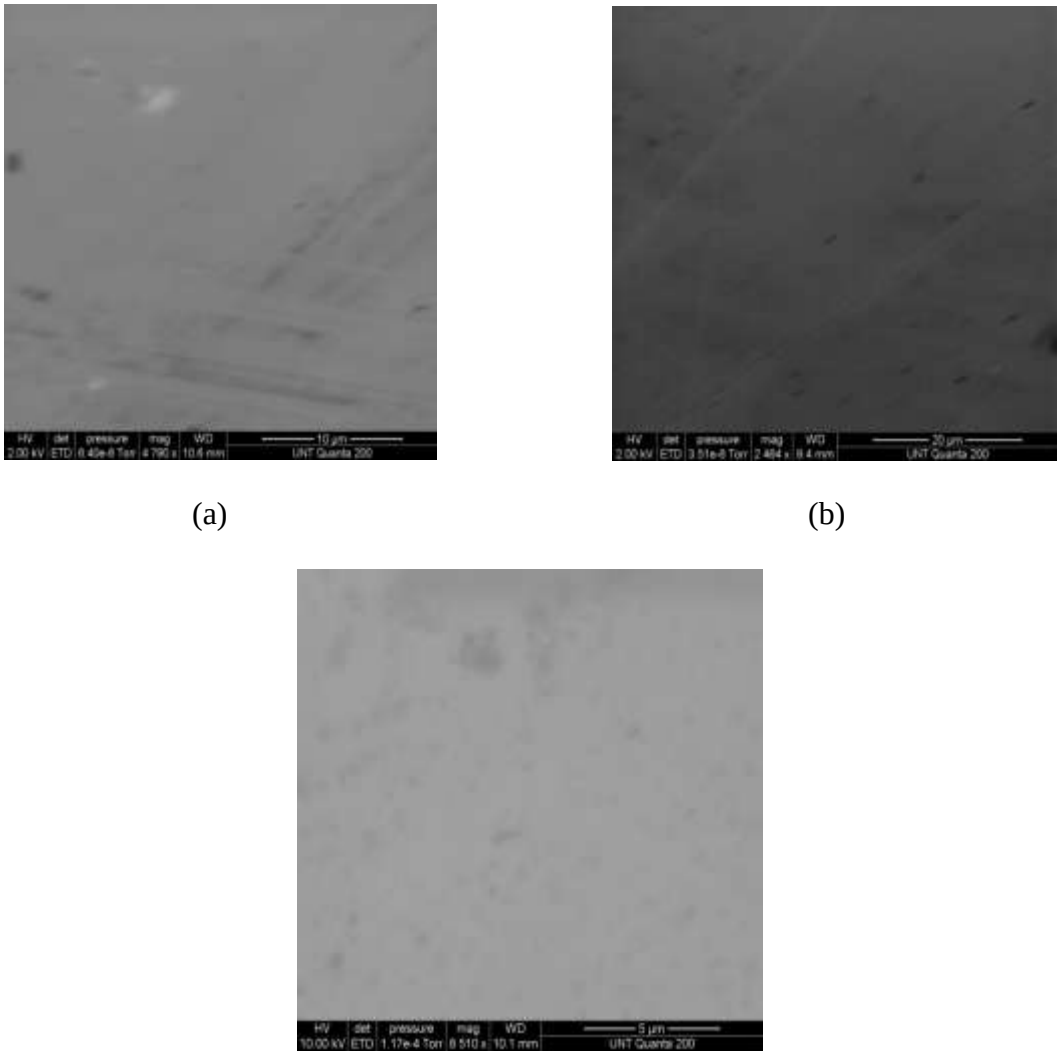

(a) (b)

(c)

Figure 22. SEM images of sample 5 (a), sample 6 (b) and sample 7 (c).

Samples deposited for 1 hour at 400°C.

The time and the temperature were increased for samples 8 and 9 to 1 hour and 400^{o}C. The deposition time for 1 hour increases the possibility of a thicker layer formation. The temperature was kept at 400^{o}C in anticipation of a growth progression from a hexagonal to a cubic phase. Deposition parameters are described in Table 10. The FTIR and XRD techniques were applied to determine the formation of the type phase.

Table 10. Deposition parameters used for samples 8 and 9.

Deposition parameters	**Value**
Initial pressure	$4.5X10^{-7}$ torr
Working pressure	$1.2X10^{-5}$ torr
Filament current	4 amps
Emission current	57 mA
Deposition time	1 hour
Cooling water supply	20^{o}C
Substrate temperature	400^{0}C

Figure 23 (a) and (b) show infrared spectra from samples deposited for 1 hour at 400°C. According to the absorption bonds shown (Kester et al., 1994), both spectra present a hexagonal phase. Figure 23 (a) depicts hexagonal phase around the wavenumber 970 cm^{-1} and some cubic phase around its characteristics peak 1062 cm^{-1}. The transmittance peak at 1300 cm^{-1} is not present for sample 8. This peak is a characteristic from in-plane B-N stretching mode (Ulrich et al., 2006). Figure 23 (b) shows the hexagonal phase. Cubic phase around 1029 cm^{-1} is presented to a lesser proportion compared to the hexagonal phase.

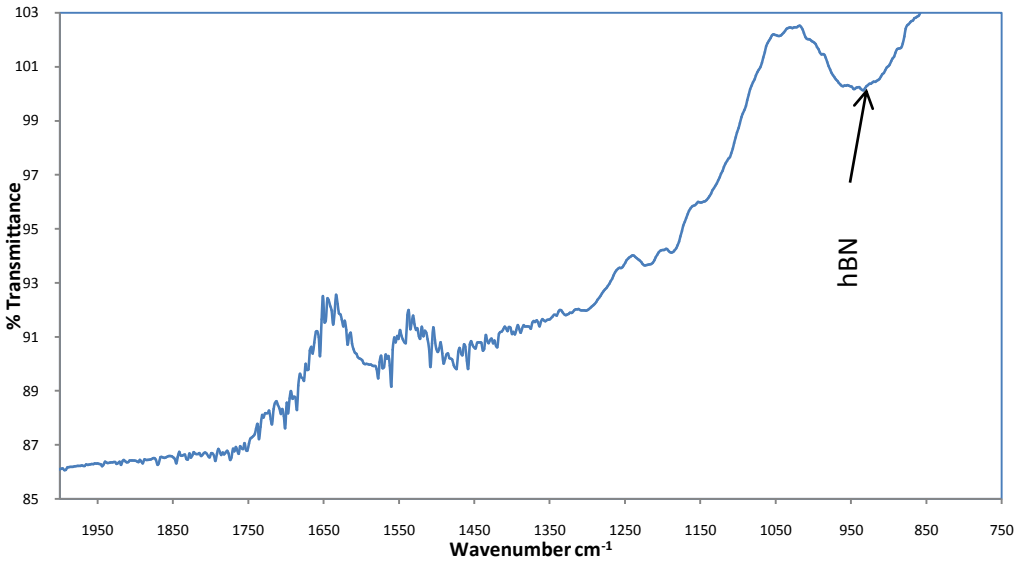

(a)

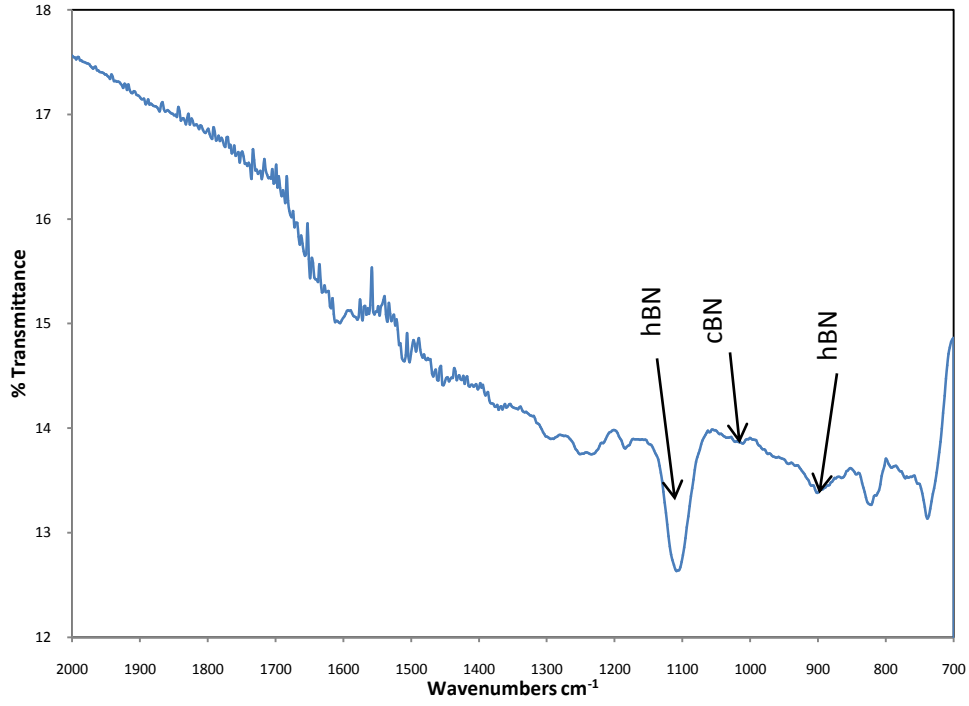

(b)

Figure 23. FTIR spectra from samples 8 (a) and 9 (b).

Figure 24 (a) for sample 8 shows diffraction from silicon substrate at 29° from (100) orientation with high intensity. Sample 8 has hexagonal phase deposited shown by the diffraction at 26° from hexagonal BN (002). Figure 24 (b) for sample 9 depicts a high peak for silicon (400) diffraction at 69° C and cBN (111) diffraction at 43° as reported in the literature (Samantaray et al., 2005 and Tian et al., 2000).

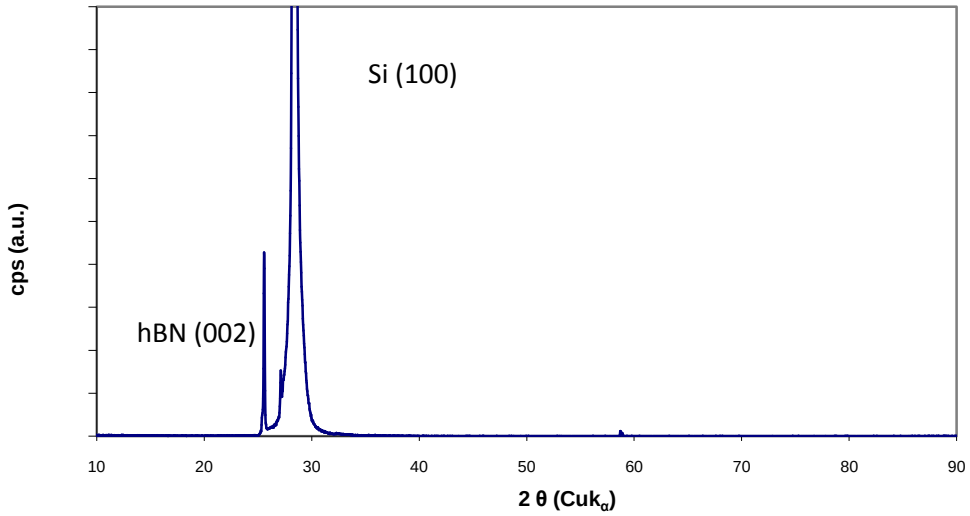

(a) Sample 8

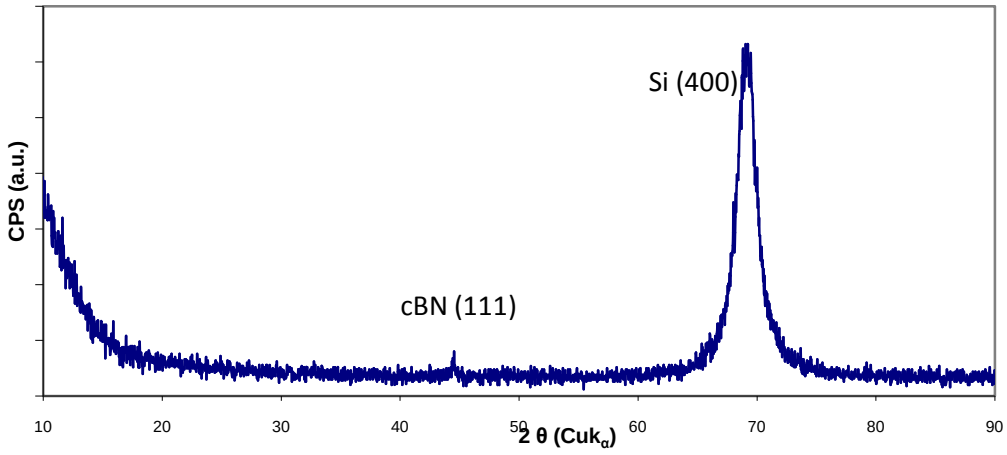

(b) Sample 9

Figure 24. XRD spectra from sample 8 (a) and sample 9 (b) deposited for 1 hour at 400°C.

Figure 25 (a) is the energy dispersive spectrum for sample 8. Boron emissions are not present as high as counts for carbon or oxygen. Nitrogen is in less intensity than boron at 0.185 keV and 0.392 keV principal emissions, respectively. SEM image for sample 8 shows scratches on the surface, which is mainly hexagonal phase based in FTIR and XRD analysis.

Figure 25 (c) shows an EDS from sample 9 deposited for 1 hour at 400°C. Boron principal emission are present at 0.185 keV with high counts. Though there are high counts for boron, nitrogen counts at 0.392 keV are not high. Carbon and oxygen are present with high counts. Figure 24 (d), SEM image, shows poruos formation over the surface, which is a sign of phase formation accordign with infrared and diffraction analysis.

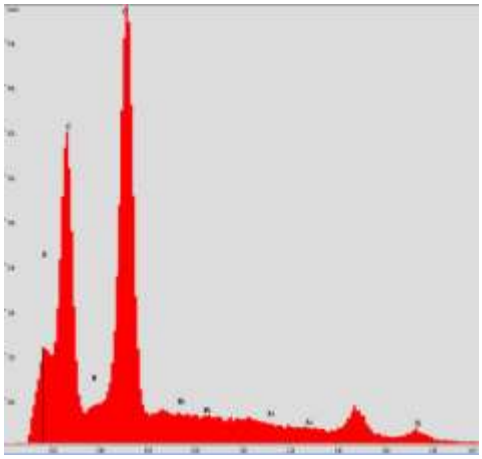

a) EDS sample 8

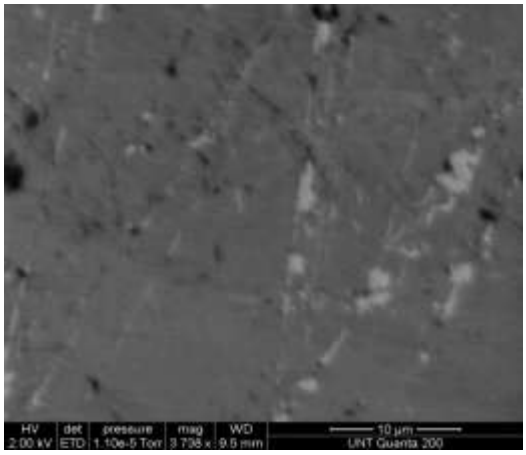

b) SEM image sample 8

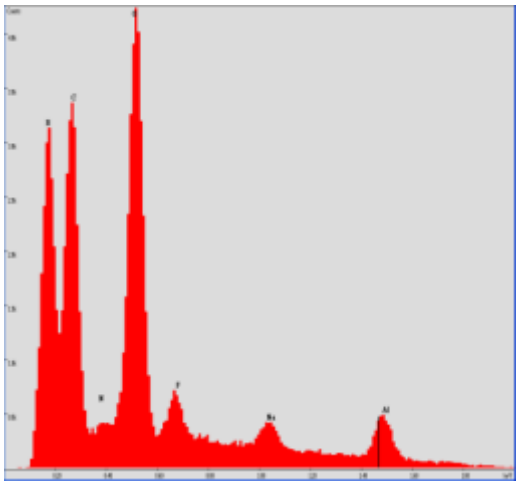

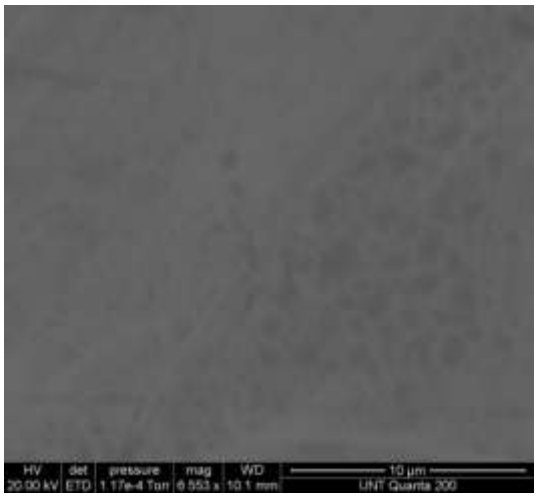

c) EDS sample 9 d) SEM image sample 9

Figure 25. EDS and SEM from sample 8 (a,b) and sample 9 (c,d) deposited for 1 hour at 400° C.

TEM samples were obtained by lift-out procedure described in chapter III. TEM images from sample 9 expose three components: silicon (substrate), BN (film) and platinum. The silicon area is clearly differentiable from the BN film. The substrate is the source for the diffraction shown in Figure 23 for silicon (400). The boron nitride film is measured by ImageJ (software). The thickness of the BN film for sample 9 is around 31.9 nm. The deposition time and the temperature had influenced the cubic phase formation, however, the FTIR and XRD results show hexagonal and cubic phase thus it can be assumed that the thicknes shown in Figure 26 is mainly hexagonal.

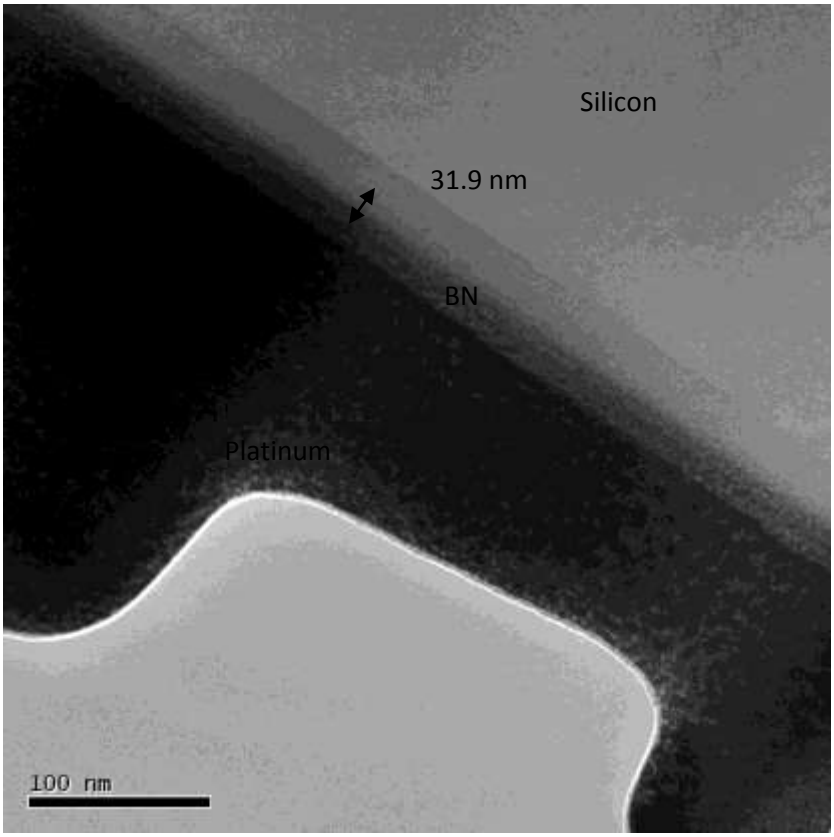

Figure 26. TEM micrograph for sample 9 that was deposited for 1 hour at 400°C at 3400X magnification.

The AFM , Figure 27, shows a 11.6 nm thickness with a root mean square (rms) surface roughness of 19 nm. The rms roughness provides information about the deposition process and thickness (He et al., 2005). The deposition process uniformity is correlated with the roughness, while the thickness is related with the surface roughness. Sample 9 with 19 nm rms roughness indicates film growth on the substrate.

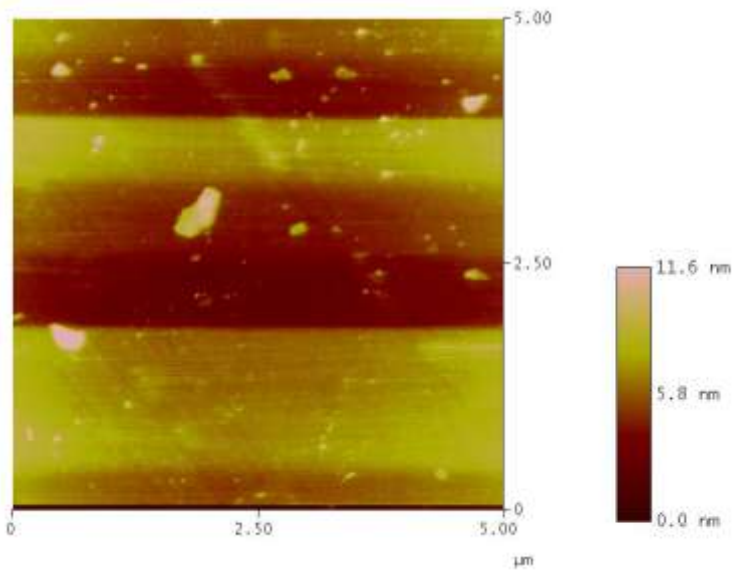

(a)

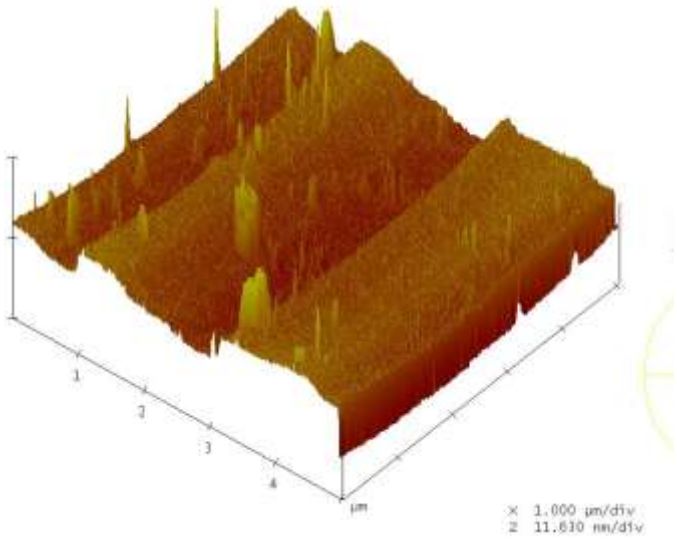

(b)

Figure 27. AFM image for roughness (a) and surface images (b) with 11.6 nm thickness from sample 9.

Figure 28 (a) is the section analysis obtained from the surface in Figure 28 (b). The section analized depicts the BN deposition topography over the the silicon substrate. The uniformity of the BN film detailed in Figure 28 (a) provides information about the surface

roughness within a range of 5.5 nm. Surface roughness is of importance for electronic application.

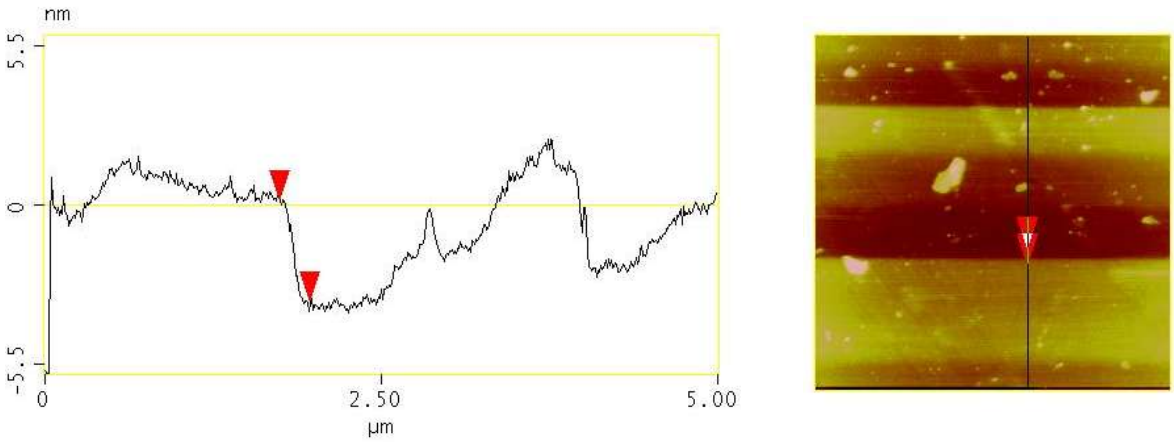

(a) (b)

Figure 28. AFM for section analysis (a) and surface image (b) for a sample deposited for 1 hour at 400°C

Sample deposited for 2 hours at 400° C.

Sample 10 was deposited for 2 hours at 400°C to determine the influence of increased deposition time on film thickness and phase formation. The deposition parameters are presented in Table 11. FTIR and XRD are techniques to characterize phase formation.

Table 11. Deposition parameters for sample 10.

Deposition parameters	**Value**
Initial pressure	$4.8X10^{-7}$ torr
Working pressure	$1.8X10^{-5}$ torr
Filament current	4 amps
Emission current	56mA
Deposition time	2 hours

Cooling water supply	20^{o}C
Substrate temperature	400^{o}C

Figure 29 (a) shows cubic phase formation. The wavenumbers in Table 4 for cubic phase are present in the spectrum at 1050 cm^{-1} and 1340 cm^{-1}. The hexagonal characteristics bonds are also present. The infrared spectrum for sample deposited for 2 hours at 400°C shows higher amount of cubic phase than depositions with less time and same temperature. Though there is cubic phase present in the deposition, the hexagonal phase presence is more pronounced in the sample. Figure 29 (b) shows a high intensity peak at 44^{o} that is the diffraction from a cBN (111). A silicon (400) peak at 70° from the substrate, Si (100), diffracted from the substrate is also shown.

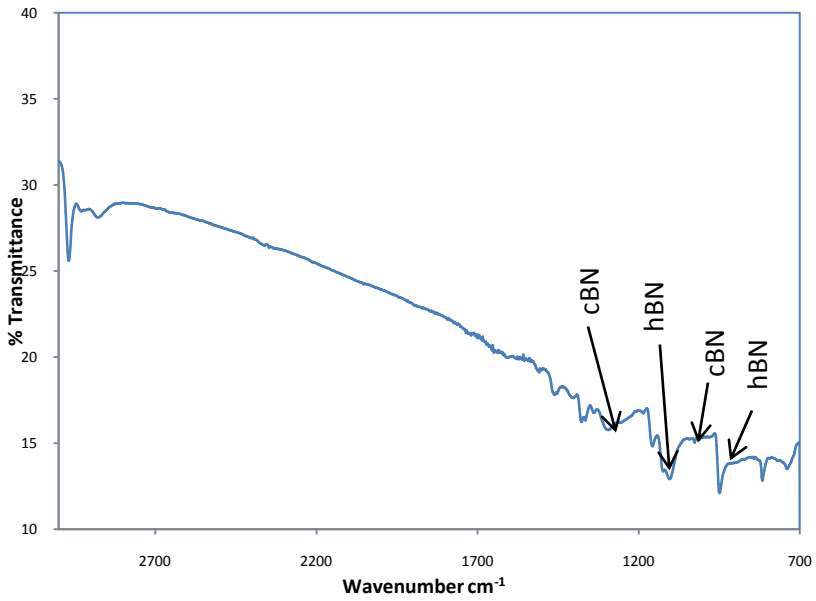

(a)

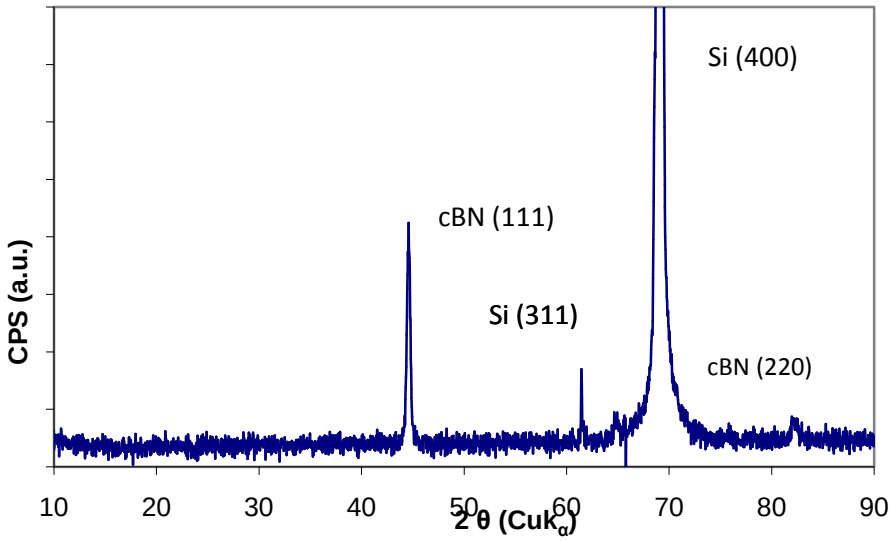

(b)

Figure 29. FTIR (a) and XRD (b) spectra from sample 10.

The energy dispersive spectrum, Figure 30 (a), indicates a principal boron emission at 0.185 keV with high counts. Nitrogen deposition is present with an emission at 0.392 keV. The carbon and oxygen emissions are also indicated in the spectrum. Figure 30 (a) shows a strong boron peak of the sample area shown in Figure 30 (b).

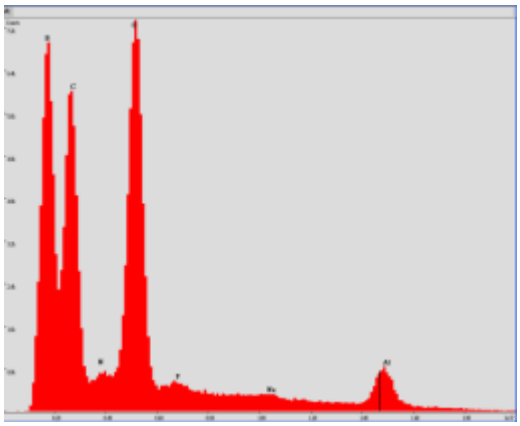

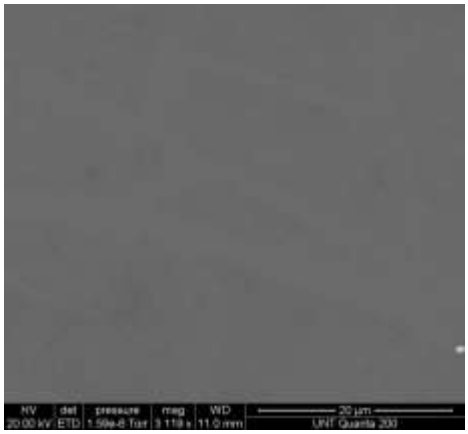

(a) (b)

Figure 30. EDS spectrum (a) and SEM image (b) from a sample deposited for 2 hours at 400°C.

The image in Figure 31 represent a cross section from sample 10 deposited for 2 hours at 400^{o}C. The thickness of the film for this deposition is 32 nm. Figure 31 shows the silicon substrate, the film and the platinum deposition. The film area can be differentiated from silicon and platinum. Formation of different phases is characteristic for the development of cubic phase (S. Ulrich et al., 2006). The thickness of the film in sample 10 and the beam spot size in the TEM prevent obtaining diffraction pattern from the area desired.

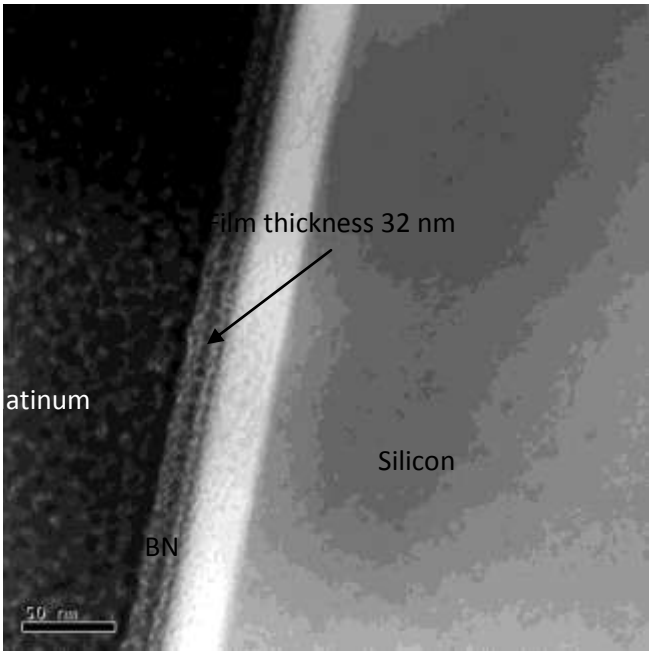

Figure 31. TEM image from sample 10 at 34000X magnification.

A cross section analysis with TEM for sample 10 deposited for 2 hours at 400^{o}C indicates the three main elements silicon, BN film and platinum. The amorphous platinum is represented by the diffraction in Figure 32. The silicon diffraction is also present in the selected area electron diffraction (SAED), which is similar to the diffraction obtained from sample 4.

The cubic diffractions patterns in Figure 33 measured with Image J show a cBN (331) with 0.085 nm and cBN (311) with 0.109 nm. These two measurements from the lattice plane spacing compare with theoretical values, 0.083 nm and 0.019 nm respectively, determine the cubic phase in sample 10 as recorded by C.B. Smantaray et al., 2005.

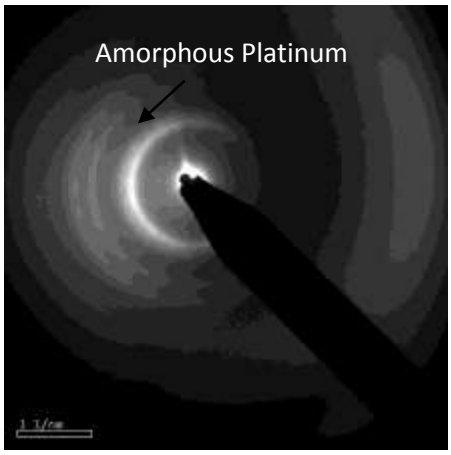

Figure 32. TEM micrograph showing amorphous platinum diffraction from sample 10.

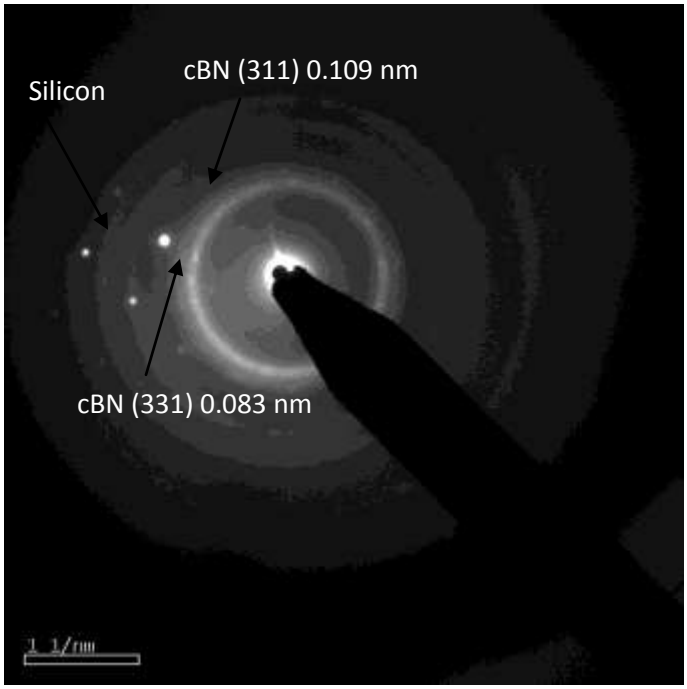

Figure 33. Film diffraction from sample 10 containing a-Pt, Si and cBN.

In the case of sample 10, a tribological performance for measurement of friction coefficient was done. Two tests were conducted, test one with 100 g of load and test two with 50 g of load at a velocity of 1.64 cm/s. Test one shows a constant friction coefficient of 0.066-0.166 and test two shows 0.071-0.105, both for 100 turns. The literature review reported friction coefficient for cBN within the range of 0.18-0.22 within 30 cycles and removal of some parts of the film (S. Miyake et al., 1992). The friction coefficient results for both tests are constant and similar within one hundred cycles, after which the friction coefficients increased. From these results the films tested show have excellent wear resistance.

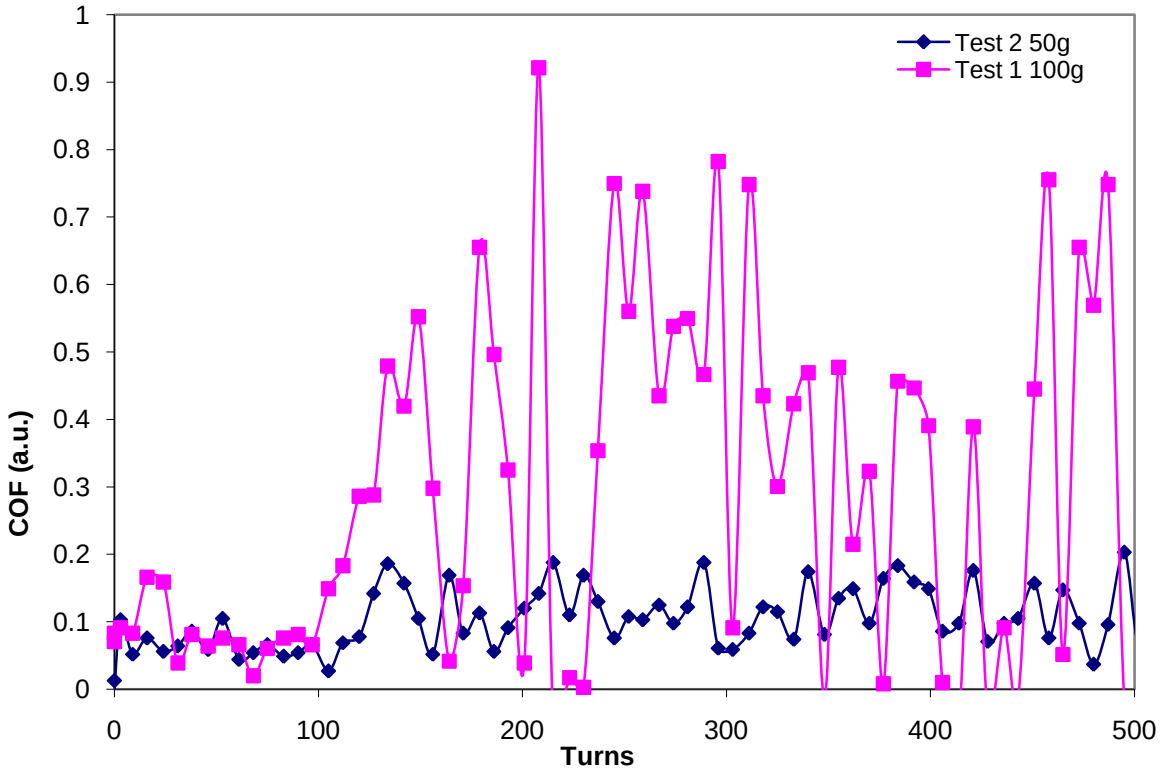

Figure 34. 52100 Steel ball on cBN film with 50g and 100g loads at 1.64 cm/s in a tribological test.

Figure 35 (a) and (b) represent the surface roughness and side perspective. The rms surface roughness obtained with AFM is 51.487 nm for sample 10. Comparing sample 10 with rms surface roughness from sample 9, 19 nm, indicates a growth in thickness. The thickness

obtained with AFM is 35 nm that is close to the results from the TEM 32 nm of thickness. The thickness increased due two hours of deposition and cubic phase is present in the thin film.

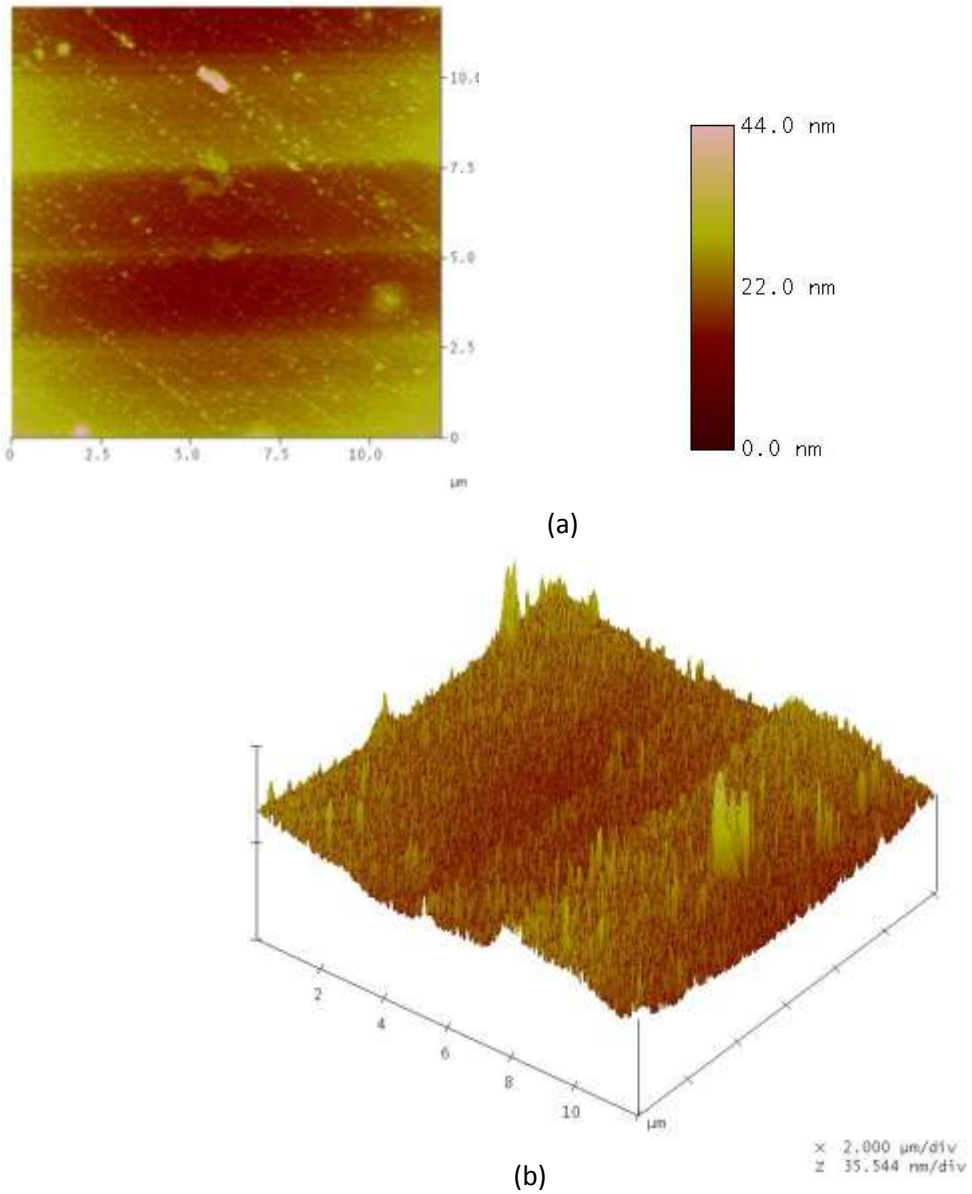

Figure 35. AFM images for roughness (a) and surface image (b) with 44 nm thickness from sample 10.

AFM section analysis in Figure 36 (a) shows surface roughness within a range of 20 nm. The deposition time had influenced the film thickness and phase formation. The surface shows a

smooth film without the trench shape in samples deposited for 1 hour. Peaks formed by the BN deposition are of the interest in field emission studies.

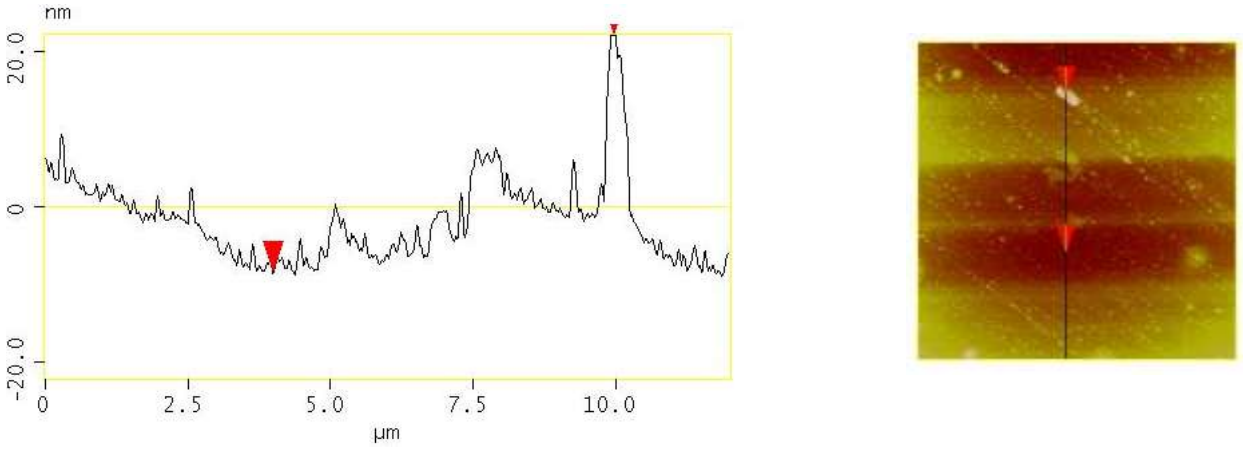

(a) (b)

Figure 36. AFM for section analysis (a) and surface image (b) for a sample deposited for 2 hours at 400°C.

CHAPTER V

CONCLUSIONS

Received samples of silicon (100) wafers containing BN film deposited through electron beam evaporation method without nitrogen bombardment and applied bias voltage were fully characterized. Sample characterization with FTIR and XRD was done to determine phase formation. SEM was used to recognize surface morphology and EDS to determine elements deposited. TEM was performed to measure thickness and phase determination. AFM was applied to obtain thickness and surface roughness. The tribological test of the sample deposited for 2 hours at 400°C measured the BN film friction coefficient.

The analysis done to the samples in this investigation can be separated by parameters of time and temperature.

i) Samples deposited for half hour at room temperature were characterized by FTIR, XRD, SEM and EDS. Hexagonal phase formation is shown in the infrared spectra although diffraction spectra, surfaces images and energy dispersive spectrum showed no evidence of BN deposition. SiO_2 is present in the diffraction spectrum and high content of oxygen in the EDS spectrum. The SiO_2 diffraction could be mistaken as a sign that BN film deposited was thin and not stable and was delaminate from the substrate leaving a thin film of oxide. The deposition time and substrate temperature are not sufficient to accomplish a stable cBN phase formation.

ii) Samples deposited for 1 hour at room temperature were characterized by FTIR, XRD, SEM and TEM. The infrared spectra showed hexagonal and cubic phase formation. The absorption bonds from cubic phase are less intensive than those from the hexagonal phase. The diffraction patterns had hexagonal and cubic phase diffractions. The hexagonal phase diffraction is higher in intensity than the cubic phase diffraction. SEM image depicted layer formation on the substrate.

TEM images illustrated a BN film thickness of 15 nm. Deposition for 1 hour demonstrates hexagonal phase formation without the necessity of high substrate temperature. Cubic phase is accomplished with these deposition parameters in less proportion than hexagonal phase.

iii) Samples deposited for half hour at 400°C were characterized by FTIR, XRD, SEM and EDS. The infrared spectra showed hexagonal phase without cubic phase. XRD spectra, surface images with SEM and the EDS spectra exhibited no indication of BN phases formation. The samples deposited for half hour demonstrated longer time is essential that is essential for hexagonal phase formation.

iv) Samples deposited for one hour at 400°C were characterized by FTIR, XRD, SEM, EDS, TEM and AFM. The characteristic transmittance bonds in the infrared spectra for hexagonal and cubic phases are more recognizable. XRD spectra showed higher intensity from cubic diffractions. SEM images exhibited film formation over the substrate and EDS spectra showed boron emissions. TEM image measured demonstrate a film thickness of 31.9 nm, which is the double of deposition for 1 hour at room temperature. AFM section analysis and the root mean square surface roughness demonstrate the surface smoothness and the deposition pattern. AFM images showed that the deposition for 1 hour at 400°C has created a uniform layer as base for cBN peaks. The substrate temperature influenced the cubic phase growth in the depositions.

v) Sample deposited for two hours at 400°C was characterized by FTIR, XRD, SEM, EDS, TEM, AFM and a friction test applied. Transmittance bonds from hexagonal and cubic phases are present in the IR spectrum. Diffraction characteristics confirmed the presence of hexagonal and cubic phases. XRD spectrum of this sample depicted a highly intense (111) diffraction line. Boron principal emissions in the EDS spectrum represent the high content of this element in the sample depositions. SEM image exhibits porous formations to be considered as significant

evidence of film growth. TEM image showed a thickness of 32 nm that is constant throughout the lift-out sample length. The process to obtain the TEM sample could have affected the final measured thickness due the platinum deposition. SAD pattern showed what silicon and platinum diffraction as expected. Cubic boron nitride diffraction pattern is also established in the TEM image. AFM surface roughness (rms) and section analysis depicted a rough surface due the deposition time and substrate temperature. Friction test results showed good friction coefficient properties. The results from the different deposition parameters combinations are summarized in Table 12.

Table 12. Characterization comparing table for samples with BN deposition

Samples		**FTIR**	**XRD**	**SEM**	**EDS**	**TEM**	
Time (hrs)	**Temperature (°C)**					**Thickness (nm)**	**Diffraction phase**
1/2	Room temperature	Hexagonal phase, SiO_2	Silicon diffractions	No indication of phases	Boron emission		
1	Room temperature	Hexagonal and cubic phase	Hexagonal and cubic diffractions	Some formation	No emission	15nm	cBN
1/2	400°C	Hexagonal phase	Silicon diffraction	No formation	No emission		
1	400°C	Hexagonal and cubic phase	Hexagonal and cubic diffraction	Poruos formation	Boron emission	31.9 nm	
2	400°C	Hexagonal and cubic phase	Hexagonal and cubic diffraction	Layer formation	Boron emission	32 nm	cBN

CHAPTER VI

FUTURE WORK

Deposition samples were manufactured by previous work and new samples were not possible due the limitation in equipment. Future samples can be deposited for more than two hours. Samples can be deposited for more than two hours and without substrate temperature. Measure thickness and phase formation from samples to determine hexagonal phase development. The information of hexagonal phase formation will define at what stage to apply substrate temperature to achieve cubic boron nitride phase.

An interesting analysis could be done at the phases interlayer to define the transformation from hexagonal to cubic phase. The direction of the hexagonal layer is important for cubic growth, thus a High Resolution Scanning Transmission Electron Microscopy (HRSTEM) will illustrate the growth orientation.

To achieve a uniform film, physical deposition parameters have to be investigated. The improvement of sample holders and distance between e-beam gun and sample is important to insure the deposition. Gas contaminants have to be measured to achieve high quality films. Contaminants during the deposition process could influence the deposition quality.

REFERENCES

Abendroth, B., Gago, R., Eichhorn F., & Moller,W.(2004). X-ray diffraction study of stress relaxation in cubic boron nitride films grown with simultaneous medium-energy ion bombardment. *Apply Physics Letter 85 (24),* 5905- 5907.

Bhushan, B. (2002). *Introduction to Tribology*. New York: John Wiley & Sons.

Brundle,C. R., Evans, C. A., Jr. & Wilson, S.(1992). *Encyclopedia of Materials Characterization*, Greenwich, CT: Manning Publications.

Bundy, F. P., & Wentorf, R. H. (1963). Direct transformation of hexagonal boron nitride to denser forms. *Journal of Chemical Physics, 38 (5),* 1144-1149.

Chong, Y. M., Leung, K. M., Ma, K. L., Zhang, W. J., Bello, I., & Lee, S. T. (2006). Growing cubic boron nitride films at different temperatures. *Diamond & Related Materials, 16,* 1155-1160.

Chowdhury, M. P., & Pal, A. P. (2004). Synthesis of cubic boron nitride film by inductively coupled plasma CVD technique. *Applied Physics, 37*, 261-268.

Deng, J., & Chen, G. (2006). Surface properties for cubic boron nitride thin films. *Applied Surface Science, 252 (22),* 7766-7770.

DoITPo Teaching and Learning Packages. *X-ray diffraction*. Retrieved March 2007, from University of Cambridge Web site: http://www.doitpoms.ac.uk/tlplib/xray-diffraction/bragg.php

Samantaray, C. B., & Singh, R. N. (2005). Review of synthesis and properties of cubic boron nitride thin films. *International Materials Reviews, 50,* 313-344.

Djouadi, M. A., Banakh, O., Soltani, A., Sanjines, R., & Levy, F. (2001). Physical properties of cubic boron nitride films synthesized by PVD using a bi-step process. *Thin Solid Films, 398,* 205-209.

Elshabini Riad, A, & Barlow, F.D.,III. (1998). *Thin film Technology Handbook*. New York:McGraw-Hill.

Feldermann, H., Ronning, C., & Hofssas, H. (2001). Cubic boron nitride thin film heteroepitaxy. *Journal Apply Physics*, 90, 3248-3254.

Freund., L.B., & Suresh, S. (2003). *Thin film materials stress, defect formation and surface evolution.* United Kingdom, Cambridge: Cambridge University Press.

George, J. (1992). *Preparation of thin film.* New York: Marcel Dekker Inc.

Gimeno, S., Munoz, J. C., & Lousa, A. (1998). Deposition time influence on cubic boron nitride thin films by tuned rf magnetron sputtering. *Thin Solids Films, 317,* 376-379.

Glocker, D. A., & Ismat Shah, S. (1995). *Handbook of thin film process technology.* Philadelphia, PA: Institute of Physics Publishing.

Grigoriew, H., & Leciejewicz, J. (1989). X-ray and electron microscopy study of amorphous boron nitride films. *Thin Solid films, 172,* 75-79.

He, Q., Li, C., Frankel,C., Pilione, L., Drawl, B., Lu F., & Messier, R.(2005). Deposition of c-BN on silicon substrate coated with diamond thin films. *Thin Solids Films*, 96-102.

Huang, J., & Zhu, Y. T. (2000). Advances in the synthesis and characterization of Boron Nitride, *Defects and Diffusions Forum, 186-187,* 1-32.

Kester, D. J., & Messier, R. (1992). Phase control of cubic boron nitride thin films. *Journal Apply. Physics, 72(2),* 504-512.

Kester, D. J., Ailey, K. S., & Davis, R. F. (1994). Deposition and characterization of boron nitride thin films. *Diamond Related Materials, 3,* 332-336.

Kester, D. J., Ailey, K. S D., Lichtenwalner, J., & Davis, R.F. (1994). Growth and characterization of cubic boron nitride thin films. *Journal Vacuum Science Technology, A12(6),* 3074.

Kobayashi, Y., Nakamura, T., Akasaka, T., Makimoto, T., & Matsumoto, N. (2007). Hexagonal boron nitride on Ni (111) substarate grown by flow rate modulation epitaxy. *Journal of Crystal Growth,* 325-327.

Le, Y. K., & Oechsner, H. (2003). On the influence of substrate temperature for cubic boron nitride growth. *Thin Solids Films, 437,* 83-88.

LeGodec, Y., Martinez-Garcia, D., Solozhenko, V.L., Mezouar, M., Syfosse, G., & Besson, J. M. (2000). Compression and thermal expansion of rhombohedral boron nitride at high pressures and temperatures. *Journal of Physics and Chemistry of Solids, 61,* 1935-1938.

Lii, D. F., Huang J. L., Tsui, L. J., & Lee, S. M. (2002). Formation of BN films on carbon fibers by dip-coating. *Surface and Coating Technology, 150,* 269-276.

Linss, V., Rodil, S. E., Rodil, P., Reinke, P., Garnier, M. G., Oelhafen, P., Kreissig, U., & Richter, F. (2004). Bonding characteristics of DC magnetron sputtred B-C-N thin films investigated by Fourier-transformed infrared spectroscopy and X-ray photoelectron spectroscopy. *Thin Solid Films, 467,* 76-87.

Mattox, M. D. (1998). *Handbook of physical deposition processing*. New Jersey: Noyes 1998.

Mirkarimi,P. B., McCarty, K. F., & Medlin, D. L. (1997). Review of advances in cubic boron nitride film synthesis. *Material Science Engineering, 21,* 47-100.

Miyake, S., Wanatabe, S., Murakawa, M., Kaneko, R., & and Miyamoto, T. (1992). Tribology study of cubic boron nitride film. *Thin Solids Films, 212,* 262- 266.

Moller, J., Reiche, D., Bobeth, M., & Pompe, W. (2002). Observation of boron nitride thin film delamination due to humidity. *Surface Coatings and Technology, 150,* 8-14.

Nasrazadani, S., & Vemuri, P. (2005). Synthesis of cubic boron nitride thin films on silicon substrate using electron beam evaporation. *AIP Conference Proceedings, 788,* 501-506.

Nose, K., Yang, H. S., Oba, H., & Yoshida, T. (2005). Defect-induced electronic conduction of tBN thin films, *Diamond & Related Materials, 14,* 1960-1963.

Oechsner, H. (2006). Growth conditions of the cubic phase cBN in boron nitride films. *Thin Solid Films, 515,* 33-38.

Ooi, N., Rajan, V., Gottlieb, J., Catherine, Y., & Adams, J. B. (2006). Structural properties of hexagonal boron nitride: Modelling Simulation. *Materials Science Engineering, 14*, 515-535.

Sell, K., Ulrich, S., Nold, E., Ye, J., Leiste, H., Stuber, M., & Holleck, H. (2003). The constitution and properties of cubic boron nitride thin films a comparative study on the influence of bombarding ion energy. *Surface and Coatings Technology, 174-175*, 1121-1125.

Tian, L., Pan, J., He, Q., & Xu, Z. (2000). Structural characteristics of boron nitride thin films synthesized by the technique of unequal-potential hollow-cathode effect. *Surface and Coatings Technology, 131*, 70-72

Ullmann, J., Baglin, J.E.E., & Kellock, A.J. (1998). Effects of MeV ion irradiatiom of thin cubic boron nitride films. *Journal of Apply Physics, 83(6)*, 2890.

Ulrich, S., Nold, E.,Sell, K., Stuber, M., Ye, J., & Zieber, C. (2006). Constitution of thick oxygen-containing cubic boron nitride films. *Surface & Coatings Technology, 200*, 6465-6468.

Vemuri, P. (2004). *Synthesis of cubic boron nitride thin films on silicon substrate using electron beam evaporation.* Unpublished master's thesis, University of North Texas, Denton, Texas. USA.

Williams, D. B., & Carter, C. B. (1996). *Transmission Electron Microscopy Basic I*. New York: Springer Science+Business Media Inc.

Xingzhao, D., Xianting, Z., Zuoqi, H., & Yeo, A. (2002). Development of Boron Nitride coating. *Singapore Institute of Manufacturing Technology SIMTech Technical Report*, (PT/02/003/ST), 1-5.

Zhang, F., Gou, Y., Song, Z., & Chen, G. (1994). Deposition of high quality cubic boron nitride films on nickel substrates. *Apply Physics Letter, 65 (8)*, 971-973.

Zhou, Z. F., Bello, I., Kremnican, V., Fung, M. K., Lai, K. H., Li, K. Y., Lee, C. S., & Lee, S. T. (2000). Formation of cubic boron nitride films on nickel substrate. *Thin Solid Films, 368 (2)*, 292-296.

Zhou, H., Wang, R. Z., Huang, A. P., Wang, M., Wang, H., Wang, B., & Yan, H. (2002). Dependence of oriented BN films on Si (100) substrate temperature. *Journal of Crystal Growth, 241*, 261-265.